공학석사학위논문

Hydrophilic Siloxane-capped Magnetic Nanoparticles as Separable and Reusable Draw Solute in Forward Osmosis Water Treatment

친수성 실록산을 도입하여 분리 및 재사용성을 향상시킨 자성 나노입자 유도물질 개발 및 정삼투 수처리 적용에 대한 연구

2013 년 2 월

서울대학교 대학원

재료공학부

안 효 원

공학석사학위논문

Hydrophilic Siloxane-capped Magnetic Nanoparticles as Separable and Reusable Draw Solute in Forward Osmosis Water Treatment

친수성 실록산을 도입하여 분리 및 재사용성을 부여한 자성 나노입자 유도물질 개발 및 정삼투 수처리 적용에 대한 연구

지도교수 곽 승 엽

이 논문을 공학석사학위논문으로 제출함

2013년 2월

서울대학교 대학원

재료공학부

안 효 원

안 효 원 의 석사학위논문을 인준함

2013년 2월

위 원 장 장 지 영 (인)

부 위 원 장 곽 승 엽 (인)

위 원 안 철 희 (인)

ABSTRACT

Forward osmosis (FO) is an emerging technology for water treatment. Finding of feasible draw solute which is the origin of the driving force for FO is one of the most important challenges of the whole research of FO. High osmotic pressure generation and easy recycling are most required properties of draw solute. Hydrophilic magnetic nanoparticle (HMNP) has full of promise as feasible draw solute. However, gradual decline of osmotic performance after recycling process, caused by particle core aggregation, is one of the major problems of HMNP draw solute. In this work, we have synthesized HMNP capped with hydrophilic siloxane (HS-MNP) for draw solute. Be compared to the carboxylate ligands of conventional HMNP draw solutes, siloxane linkages formed by condensation of hydrophilic trimethoxysilane are considered as a good protector of particle core against aggregation on high strength magnetic fields. Ligands of MNP/oleic acid synthesized by thermal decomposition method were exchanged to hydrophilic siloxane. Two trimethoxysilanes, 2-[methoxy-(polyethyleneoxy)propyl]trimethoxysilane (Silane-PEG) and n-(trimethoxysilylpropyl) ethylenediamine triacetic acid (Silane-COOH), were used as hydrophilic ligands for HS-MNP draw solutes. Physical properties of HS-MNP draw solutes were thoroughly characterized and osmotic pressure generation of HS-MNPs were analyzed by freezing point depression osmometer. HS-MNPs were applied to a batch scale FO to determine

the water flux generation. After that, variation of water flux generation and mean particle size of HS-MNPs were measured after 5-times-repeated magnetic recycle. Osmotic pressure and water flux generation of PEG-MNP were 7.6 atm and 2.13 LMH at 0.038 mol/L of ligand concentration. Similarly, osmotic pressure and water flux generation of COOH-MNP were 6.3 atm and 1.81 LMH at same concentration. These results confirm that synthesized HS-MNPs were feasible to apply to the FO water treatment of mild brackish water or wastewater. In addition, water flux generation and particle size PEG-MNP draw solutes were well-maintained by 5-tmies of magnetic recycle. Finally, 0.038 mol/L of PEG-MNP + DI water draw solution was applied to the FO process with a feed solution with 500 ppm of methylene blue. Water flux generation with the feed solution was up to 1.58 LMH. Results of this work shows that HS-MNPs are feasible draw solutes in FO water treatment. Especially, properties of PEG-MNP as draw solute were well-maintained on magnetic recycle, and acceptable to FO water treatment of mild brackish water.

Keywords

Forward osmosis, Draw solute, Draw solution, Magnetic nanoparticle,

Hydrophilic siloxane, Water treatment

***Student number*: 2011-20649**

CONTENTS

1. Introduction

One of the most serious challenges of 21st century is to overcome the freshwater shortage. Demand of fresh water is enormously increased with the population growth and worldwide change of climate. At nowadays, billions of people lack access to feasible drinking resource. [1] Although over 70% of the earth is covered by water, usable freshwater is less than 0.8% of the whole water resource. The rest of the water is not able to be used by human because of their salinity or contamination. [2] In addition, more than half of the groundwater which is the most direct water resource for terrestrial organisms is mild brackish water. Therefore, water treatment of brackish water for widening the freshwater resource is considered to one of the most important technology for survival of human being.

Many technologies for water treatment have been developed widely. Among them, thermal separation methods and membrane separation methods are the most popular technologies for water treatment. [3] However, although their huge yield efficiency of freshwater resource, thermal separation technologies have no price competitiveness than membrane-based methods because of necessity of too much energy for heating of water. Most of membrane separation technologies have more energy efficiency than thermal separation methods. [4]

In the field of membrane-based water treatment, reverse osmosis (RO) is the

most dominant process nowadays. RO uses external hydraulic pressure to oppose the osmotic pressure of a feed solution to produce purified water. In RO, the external hydraulic pressure is the driving force for water transportation through the semipermeable membrane. A lot of publications on the use of RO for water treatment and wastewater reclamation appear in the literature. [4] [5] However, in spite of the many advantages of RO, RO has a lot of problems such as fouling, requirement of high external pressures, and low recovery efficiency only 35–50% of fresh water. [6]

Forward osmosis (FO) is one of the newest technologies for membrane-based water treatment. In FO, like RO, water moves across the semipermeable membrane. However, instead of external hydraulic pressure, a FO process utilizes an osmotic pressure gradient to induce the driving force for water transport through the membrane as shown in Figure 1. A draw solution at brine with a significantly higher osmotic pressure than the feed water flows along the permeate side of the membrane, and water naturally transport across the membrane by osmosis. [7] Based on the thermodynamics, osmotic water flow is induced by the difference of chemical potential between draw and feed solution as depicted in Figure 2. Compared to RO, FO can offer advantages including low operation pressure and temperature, potentially low fouling and less energy consumption. [8] Based on these advantages, FO has been widely researched as the technology of desalination [9] [10], wastewater purification [11], osmotic power generation [12], agricultural fertilizing [13], food processing [14], and so on.

Although the FO technology shows the great potential in water treatment, its development is challenged by a lot of problems, such as the unavailability of appropriate draw solutions which is the origin of the driving force of FO process. The main problems regarding draw solutes are the reasonable osmotic pressure and intensive energy requirement during regeneration process. Therefore, two criteria must be considered while selecting a feasible draw solution. First, high osmotic pressure for high water flux and being easy to reconcentrate the diluted draw solution which may lower energy requirement and whole operation cost. [5] [15] [16]

The one of the essential properties for any draw solute is the osmotic pressure in solution which is higher than the feed solution. The osmotic pressure of the ideal dilute solution is defined by Van't Hoff equation as shown below.

$$\pi = \mathrm{n}\left(\frac{c}{MW}\right)RT \quad \text{(Eq. 1)}$$

Where π is the osmotic pressure of the solution, n is the number of moles of species formed by the dissociation of solutes in the solution, c is the concentration in g/L of draw solution, MW is the molecular weight of the draw solute, R is the gas constant, and T is the absolute temperature of the solution. However, this equation is limited to ideal dilute solutions and is generally used for the determination of large MW.

For general solutions, the osmotic pressure is given by the concentration

dependence osmotic equation, also known as virial equation, as shown below.

$$\frac{\pi}{cRT} = 1 + Bc + Cc^2 + Dc^3 + \cdots \quad \text{(Eq. 2)}$$

Where B, C and D are the osmotic virial coefficients which are determined empirically by fitting experimental osmotic pressure data, and generally the determination of B and C is sufficient to reproduce observed data. [17] [18]

From the above equations, it is clear that, the osmotic pressure is the function of concentration of draw solutes, number of species formed by dissociation in the solution, MW of the solute and the temperature of the solution and therefore does not depend on the types of species formed in the solution. A solute with small MW combined with high water solubility can generate higher osmotic pressure and therefore can lead to higher water fluxes. [7, 18]

A wide range of draw solutes have been proposed since 1960s. Among them, inorganic salt has the majority of FO studies and they are still extensively utilized nowadays. [15] [16] [19] Specifically, McGinnis et al. were demonstrated that combining ammonia and carbon dioxide gases created thermally removable ammonium salts as draw solution. [7] [20] In this study, produced FO draw solutions induced high osmotic pressures in excess of 250 bars. However, it has some of serious drawbacks. First, although of osmotic performance of ammonia and carbon dioxide gases, its

recycle process still needs heat energy for thermal decomposition of ammonium salt at ~60 ℃. And, loss of the draw solutes caused by reverse diffusion is pointed out as a major problem of the ammonia-carbon dioxide gases.

Hydrophilic modified magnetic nanoparticle (HMNP) is recently considered as a new type of draw solutes and exhibit the advantages of extremely low reverse flux compared to traditional materials. [21] Nanoparticles with hydrophilic surface functionality and high surface area ratio can generate reasonable osmotic pressures for many of FO process. Moreover, the magnetic nanoparticles can be readily separated from a diluted draw solution by magnetic field separation. It is more efficient than the recycle process of inorganic-salt-based draw solution. However, magnetic particles are found to aggregate as larger sizes under a high strength magnetic field, causing a significant decrease in FO performance. [22] It is considered as the most serious drawback of HMNP draw solute. It is originated by carboxylate ligands of the conventional HMNP. Figure 3 describes the factor of particle aggregation of HMNPs. In conventional HMNP draw solutes with carboxylate ligands, the bonding between magnetic particle core and hydrophilic ligands is based on secondary bonding. Although it can offer sufficient dispersion stability of draw solution, it may not enough to prevent the permanent particle core aggregation by high strength magnetic field. Although some of the studies are reported to overcome this problem, [23] [24] it is remained as one of the most serious hindrance of HMNP draw solutes.

In this study, we introduced HMNPs capped with hydrophilic siloxane for a new HMNP draw solutes for FO water treatment. Siloxane is a chemical compound composed of units of the form R_2SiO, which is readily formed by condensation reaction of methoxy/ethoxysilane molecules as shown in Scheme 1. [25] The whole scheme of this study is prescribed in Scheme 2. In ligand exchange reaction, the hydroxyl functional groups (-OH) on surface of iron oxide nanoparticles attack the alkoxy groups (-OMe or –OEt) of alkoxysilane molecules. After this reaction, the covalent bondings (Fe-O-Si- and -Si-O-Si-) are formed between alkoxysilane molecules and surface of iron oxide nanoparticles. [26] Covalent bonding of Si-O-Si linkage and Fe-O-Si bonding formed by ligand exchange reaction are considered to be a good protector from particle core aggregation in high magnetic fields, Fe_3O_4 nanoparticles are considered as magnetic particle core of HMNPs by its reasonable magnetic properties for magnetic separation process, and hydrophilic branch of siloxane may generate the osmotic pressure in draw solution with HS-MNPs. MNP/hydrophilic siloxane has been synthesized by ligand exchange reaction as shown in Scheme 3. Ligands of MNP/oleic acid synthesized by thermal decomposition method have been exchanged to hydrophilic silane. During this reaction, Si-O-Si linkages have been formed by condensation of trimethoxysilane ligands. The physical properties of synthesized HMNP draw solutes were characterized by X-ray diffraction (XRD), Fourier transform infrared (FT-IR), energy-filtering transmission electron microscope (EF-TEM), electrophoretic light

scattering spectrophotometer (ELS), differential thermal analysis/thermogravimetric analysis (DTA/TGA), and freezing point depression osmometer. After that, water flux of synthesized HMNP draw solution in a batch scale FO process was measured to determine the osmotic performance. The water flux and particle size changes after each five times of magnetic separation process were measured to determine the particle stability of synthesized HMNP draw solutes. Finally, the HMNP draw solutes are applied to the FO process with brackish feed solution.

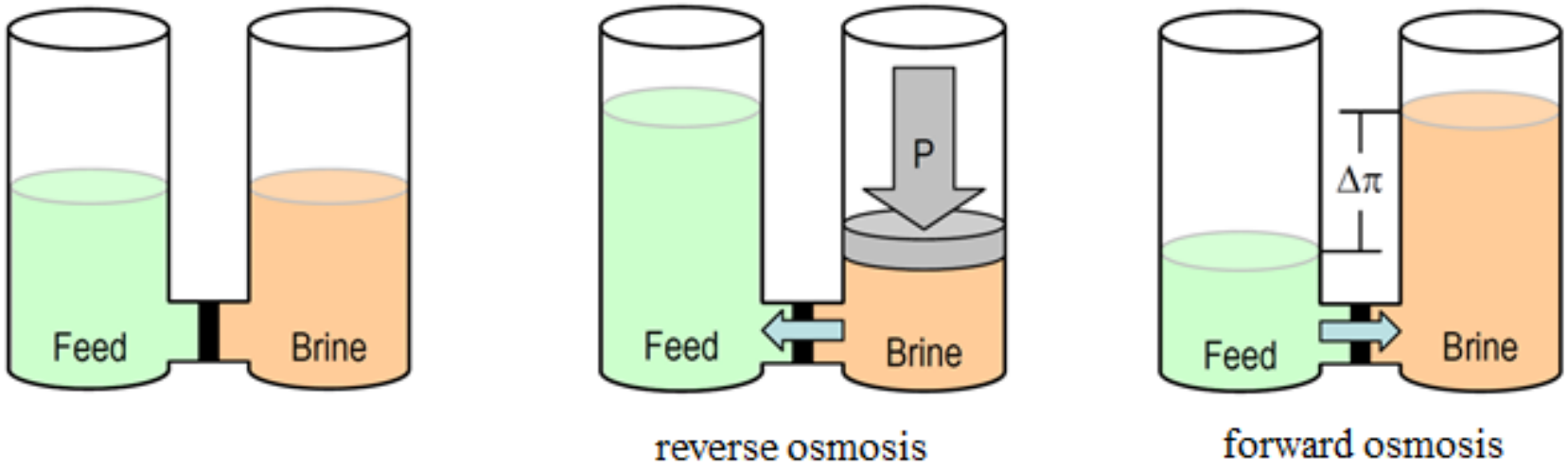

Figure 1. The principles of osmotic processes: forward osmosis (FO) and reverse osmosis (RO)

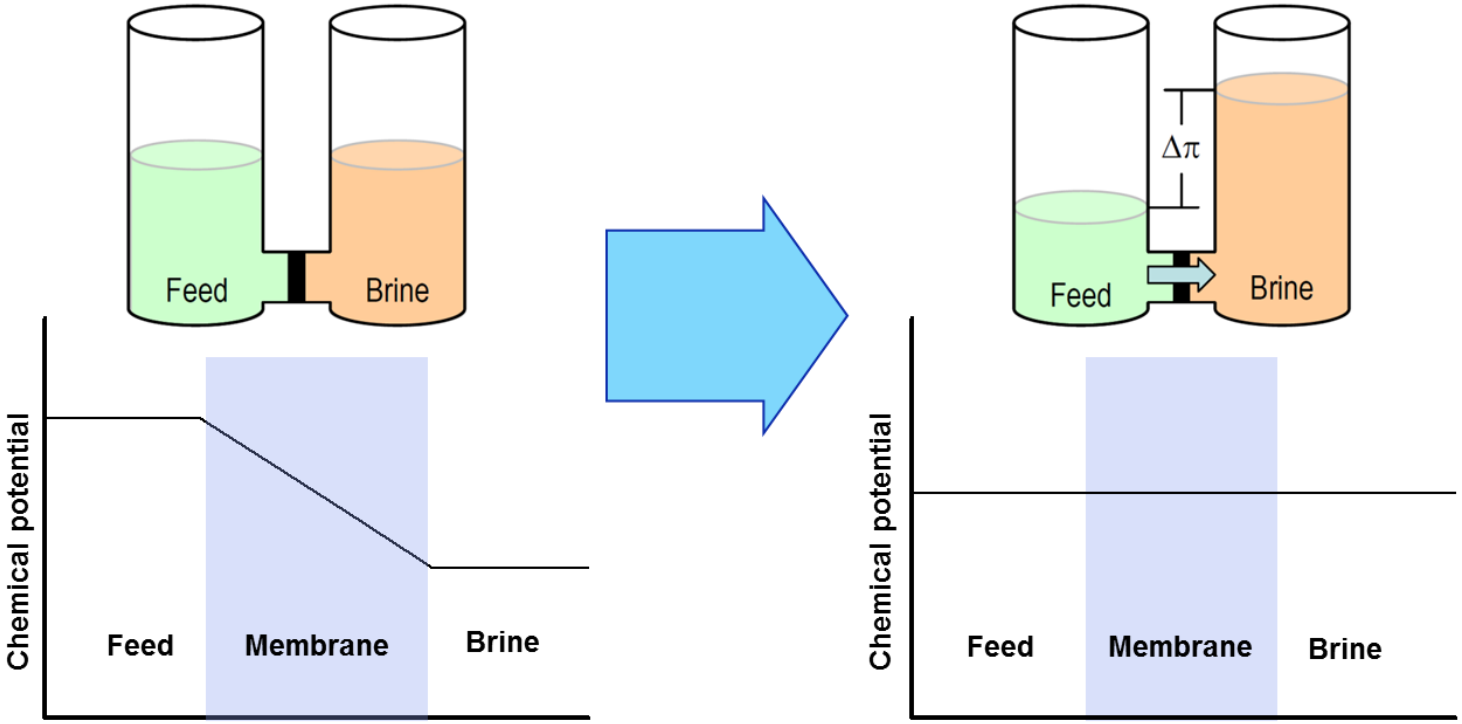

Figure 2. Spontaneous osmotic water flow induced by chemical potential gradient

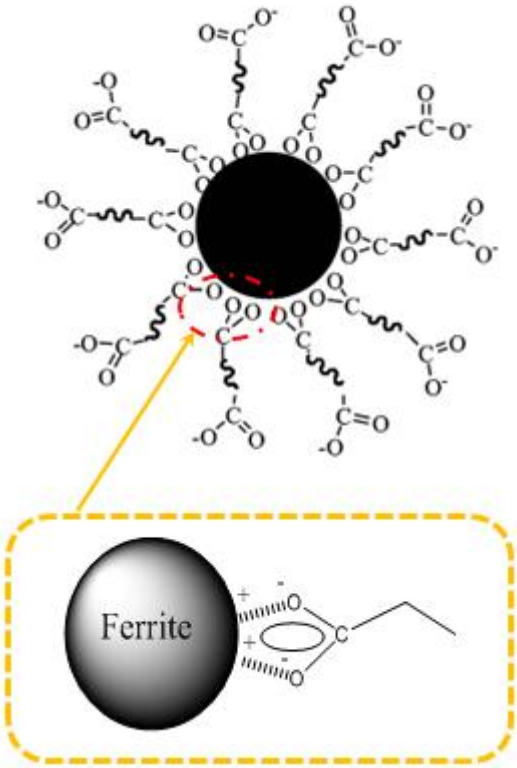

Figure 3. The factor of particle aggregation of hydrophilic magnetic nanoparticles

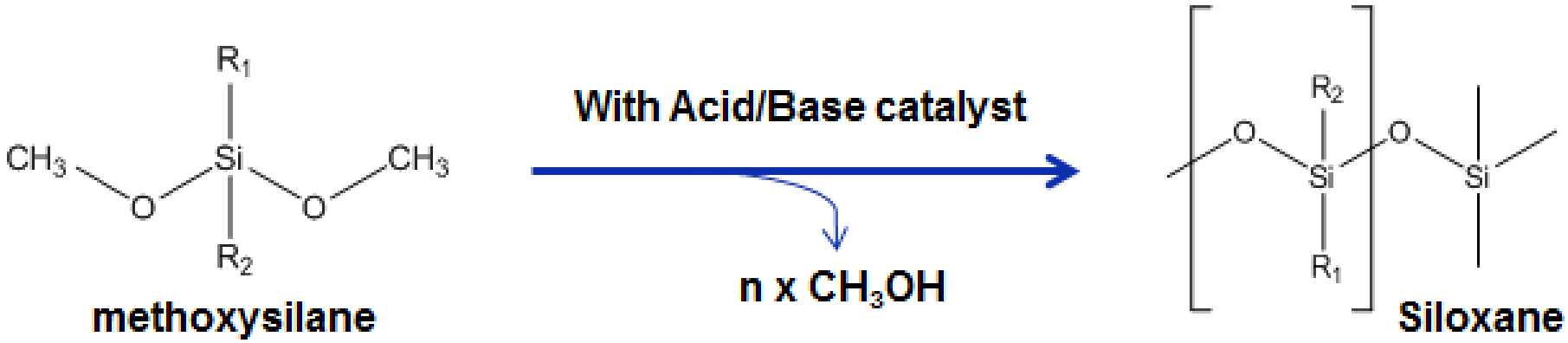

Scheme 1. Condensation reaction of methoxysilane molecules to form siloxane linkage

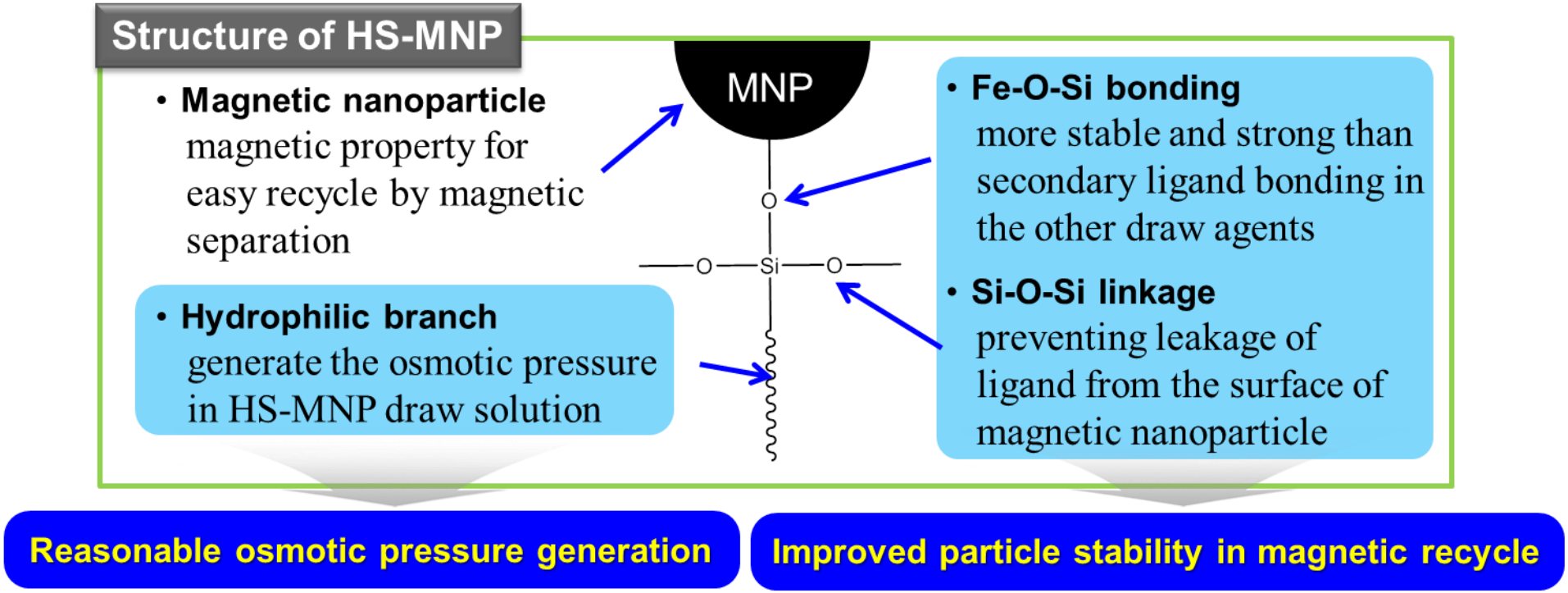

Scheme 2. Hydrophilic siloxane as a capping agent of HMNP draw solutes

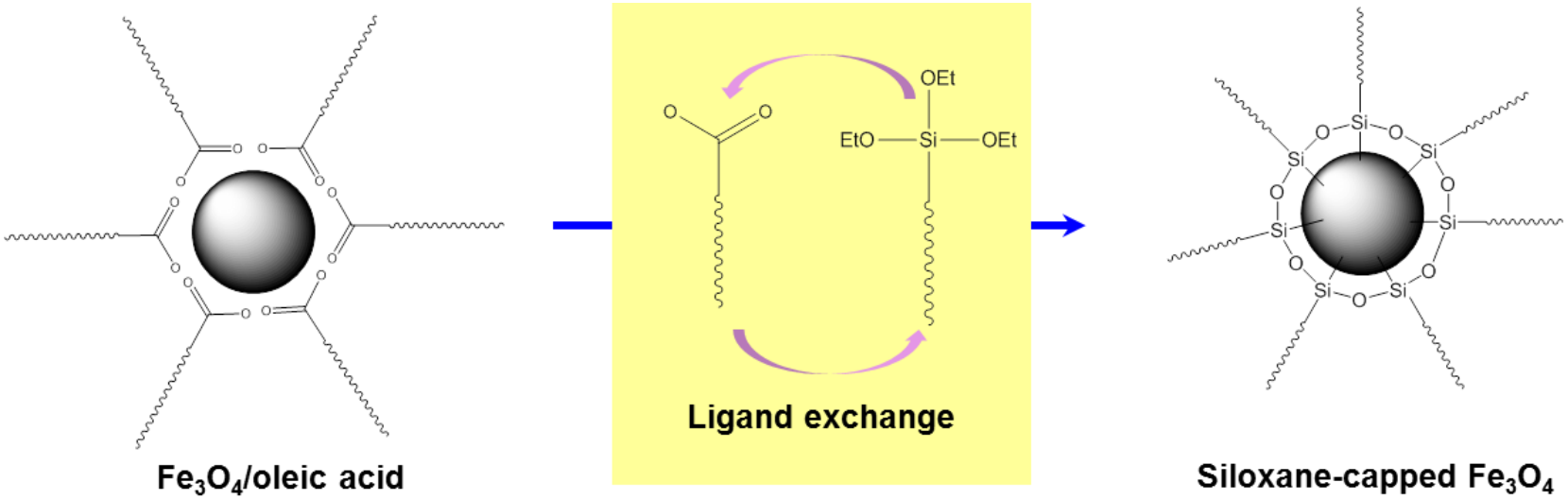

Scheme 3. Ligand exchange reaction for synthesis of HS-MNP

2. Experimental

2.1. Materials

Iron(III) acetylacetonate(97%) ($Fe(acac)_3$), oleic acid (90%), oleylamine (70%), toluene (97%), 1,2-hexadecanediol (90%), benzyl ether (99%), ethanol (99.9% anhydrous), and tetramethylammonium hydroxide(99%) (TMAH) were purchased from Sigma-aldrich. 2-[methoxy-(polyethyleneoxy)propyl] trimethoxysilane (Silane-PEG), n-(trimethoxysilylpropyl)ethylenediamine triacetic acid (Silane-COOH) were purchased from Abcr gmbh. Cellulose triacetate (CTA) membrane for FO process are purchased from Hydration Technologies Inc. (HTI) Whole materials were used as received without any additional treatment. Water used in all syntheses was distilled and deionized. (DI water)

2.2. Preparation of hydrophilic siloxane-coated magnetic nanoparticle (HS-MNP) draw solutes

Hydrophilic siloxane-coated magnetic nanoparticle (HS-MNP) draw solutes were prepared on 2 steps. First, to form a magnetic particle core, magnetic nanoparticle capped by oleic acid (MNP/oleic acid) was synthesized. After that, hydrophilic siloxane was coated to surface of nanoparticles by ligand exchange reaction.

2.2.1 Step 1: Synthesis of magnetic nanoparticle capped by oleic acid (MNP/oleic acid)

Magnetic nanoparticle capped by oleic acid (MNP/oleic acid) was synthesized by a thermal decomposition method reported by Sun et al. [27] (Scheme 3) Iron(III) acetylacetonate ($Fe(acac)_3$) 1.5 g, 1,2-hexadecanediol 5 g, oleylamine 5 mL, and oleic acid 5 mL were introduced in 40 mL of benzyl ether. The mixture was slowly heated to 200 °C for 2 h and then, under a blanket of Ar gas, heated at about 300 °C to reflux for 1 h. After that, the mixture was cooled to room temperature. To separate the nanoparticle from the mixture, 50 mL of ethanol was added to the mixture and black-brown sediment was precipitated. The precipitate was washed three times with ethanol to remove any left-over surfactants in solution. Finally, the MNPs were dispersed in toluene (300 mL).

2.2.2 Step 2: Ligand exchange reaction for hydrophilic modification of HS-MNPs

HS-MNPs were prepared by ligand exchange reaction between MNP/oleic acid nanoparticles and hydrophilic trialkoxysilanes following a arranged procedure estabilished elsewhere [28-30] (Scheme 4) Under ambient conditions, 2 mL of 2-[methoxy-(polyethyleneoxy)propyl] trimethoxysilane (Silane-PEG) and n-(trimethoxysilylpropyl) ethylenediamine triacetic acid (Silane-COOH) were added to each mixture of MNP/oleic acid nanoparticles in toluene (100 mg in 300 mL) containing 0.05 mL of tetramethylammonium hydroxide (TMAH) in a glass bottle. The mixtures were shaken for 72 h, during which the particles precipitated. The black-brown precipitate was washed three times with toluene to remove all excess silane. Finally, precipitate was redispersed in deionized water. Synthesized HS-MNPs were named as PEG-MNP and COOH-MNP derived from each of the hydrophilic branch of capping agents (Silane-PEG and Silane-COOH).

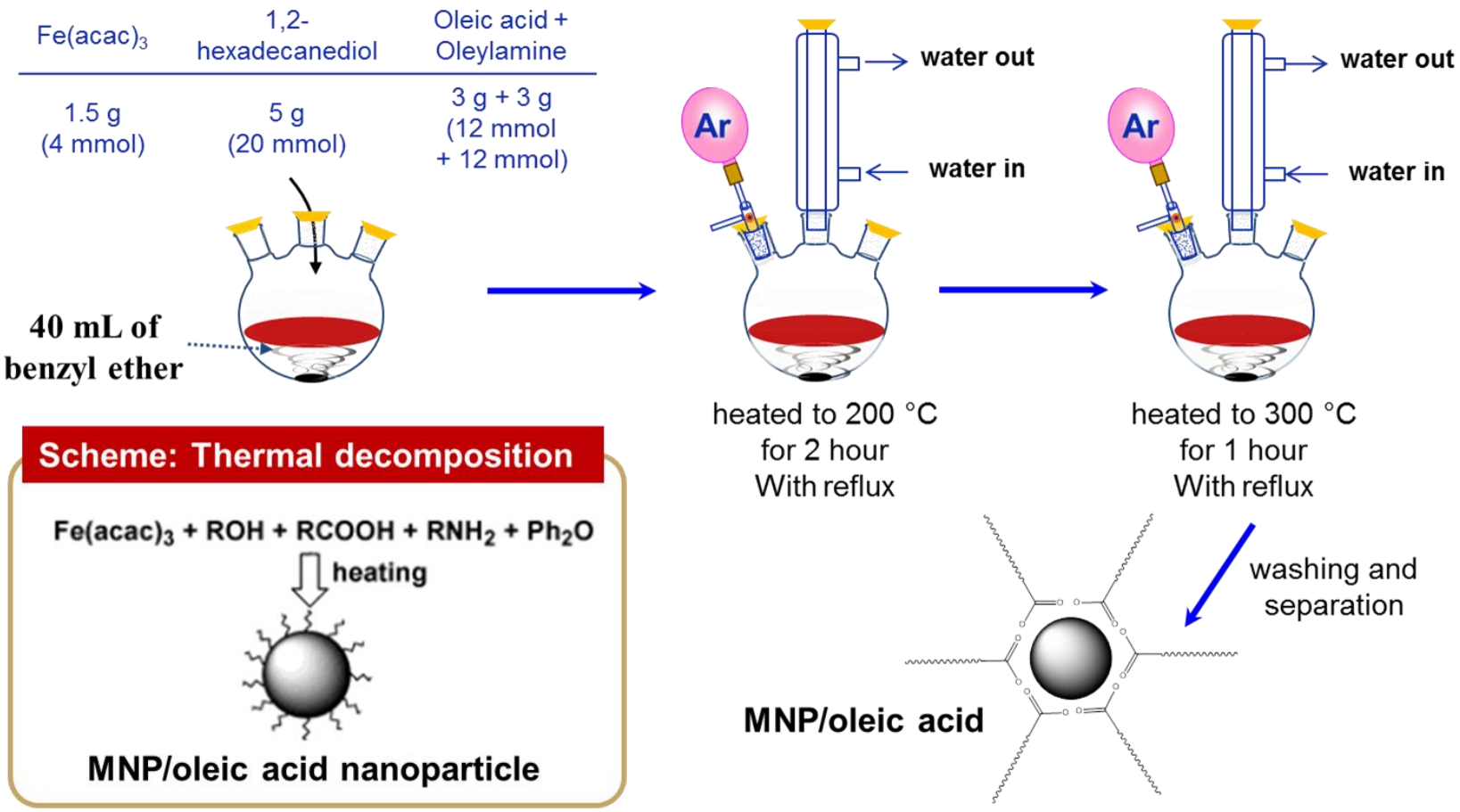

Scheme 3. The synthesis of MNP/oleic acid

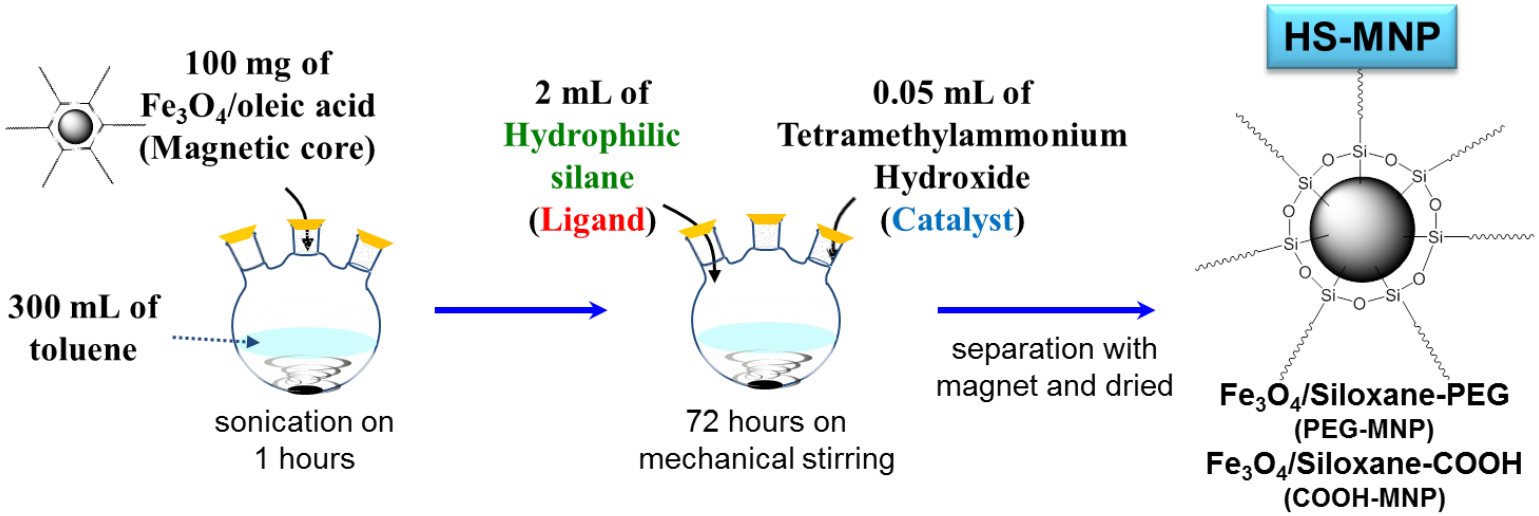

Scheme 4. Ligand exchange reaction for hydrophilic modification of HS-MNPs

2.3. Characterization of synthesized HS-MNPs

2.3.1. Crystal structure, shape and particle size distribution

The crystal structure of HS-MNPs was analyzed by X-ray diffraction (XRD) (MXP 18XHF-22SRA Diffractometer) equipped with graphite monochromatized Cu Kα radiation (λ = 1.541 Å, 50 kV, 100 mA) as the X-ray source. Scans were recorded for 2Θ values between 15° and 80° with a scanning speed of 5 min^{-1}.

The shape and size distribution of MNP/oleic acid nanoparticles and HS-MNPs were observed with energy-filtering transmission electron microscope (EF-TEM) (Carl Zeiss LIBRA 120) with ×200,000 of maximum magnification. Samples for the EF-TEM experiments were prepared by dispersing dried samples in n-hexane (MNP/oleic acid) and DI water (HS-MNPs). Particle size distribution of HS-MNPs were analyzed with Otsuka Electronics ELSZ-1000 electrophoretic light scattering spectrophotometer (ELS). Each samples for ELS analysis were prepared by dispersing under 1 mg of nanoparticles in 5 mL of DI water.

2.3.2. Surface modification of hydrophilic siloxane

Qualitative evidence of surface modification by ligand exchange reaction was analyzed by Fourier transform infrared (FT-IR) (Thermo Scientific Nicolet 6700 IR) spectra in the range 4000 to 600 cm^{-1} with was 4 cm^{-1} of spectral resolution in experiment. Samples for the FT-IR analysis were dried overnight at 50 ℃ in a vacuum prior to KBr pellet fabrication.

Quantitative evidence of surface modification was determined by results of simultaneous differential thermal analysis/thermogravimetric analysis (DTA/TGA) (TA Instruments). About 10 mg of each sample was dried in vacuum overnight at 50 ℃ to remove all solvent. Next the samples were heated from 20 ℃ to 800 ℃ at 20 ℃/min under flowing N_2 environment.

2.3.3. Osmotic pressure generation

Osmotic pressure of HS-MNP draw solutes are analyzed by freezing point depression osmometer (KNAUSER Semi-micro osmometer K-7400). Each samples for the osmometry were dispersed in under 1 mL of DI water and sonicated in water bath for 1 hour.

2.4. Forward osmosis (FO) with HS-MNP draw solutes

Synthesized HS-MNP draw solutes are applied to a batch scale of FO process as depicted in Figure 4. Concept of the batch scale FO process is shown in Figure 5. Experimental condition and measurement factor in FO process and is shown in Table 1 and Table 2.

2.4.1. Water permeation test with DI water feed solution

In this batch scale FO, DI water as a feed solution and draw solution with HS-MNPs were positioned to opposing sides of an FO membrane (HTI flat sheet CTA membrane, 2.54 cm^2). The membrane's active layer was oriented towards the feed solution and the support layer oriented towards the draw solution. Fresh membranes were soaked in deionized water for 1 hour prior to their introduction to the FO process. During the experiment, volume increase of the permeated water was measured at every 30 minutes. The feed and draw solutions were maintained at room temperature.

2.4.2. Magnetic recycling and regeneration of HS-MNP draw solutes

After FO process, HS-MNPs were separated from diluted draw solution by magnetic separation with permanent magnet as shown in Figure 6. Magnetic field strength of magnet is over 13000 gauss (on surface). Magnetically separated HS-MNPs were washed with DI water and dried in vacuum at room temperature over 12 hours. After that, recycled HS-MNPs were redispersed to DI water for reuse to the next FO process. Magnetic recycle process was repeated 5 times for each HS-MNP draw solutes. After each recycle, particle mean size of HS-MNPs was analyzed by EF-TEM and ELS to determine the variation of particle size distribution during magnetic separation.

2.4.3. Water permeation test with methylene blue feed solution

To determine the FO performance on water treatment with mild brackish water, PEG-MNP draw solute was applied to the FO process with a brackish feed solution which was prepared by addition of 500 ppm of methylene blue to the DI water. Water flux was measured during the FO process and compared to the water flux with DI water feed.

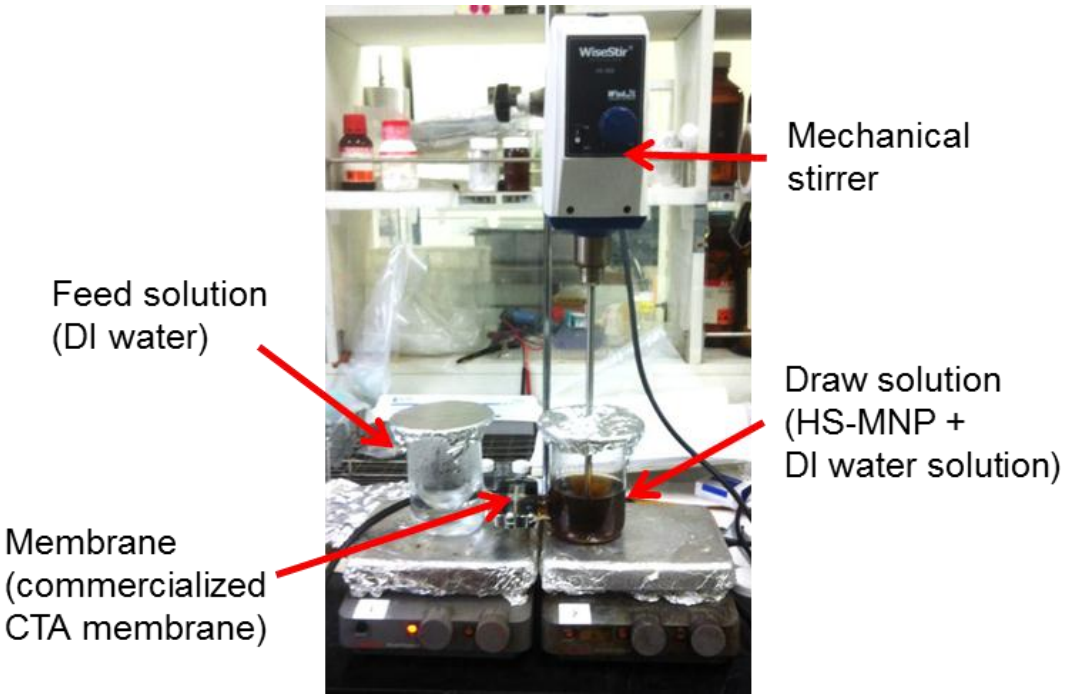

Figure 4. a batch scale FO process

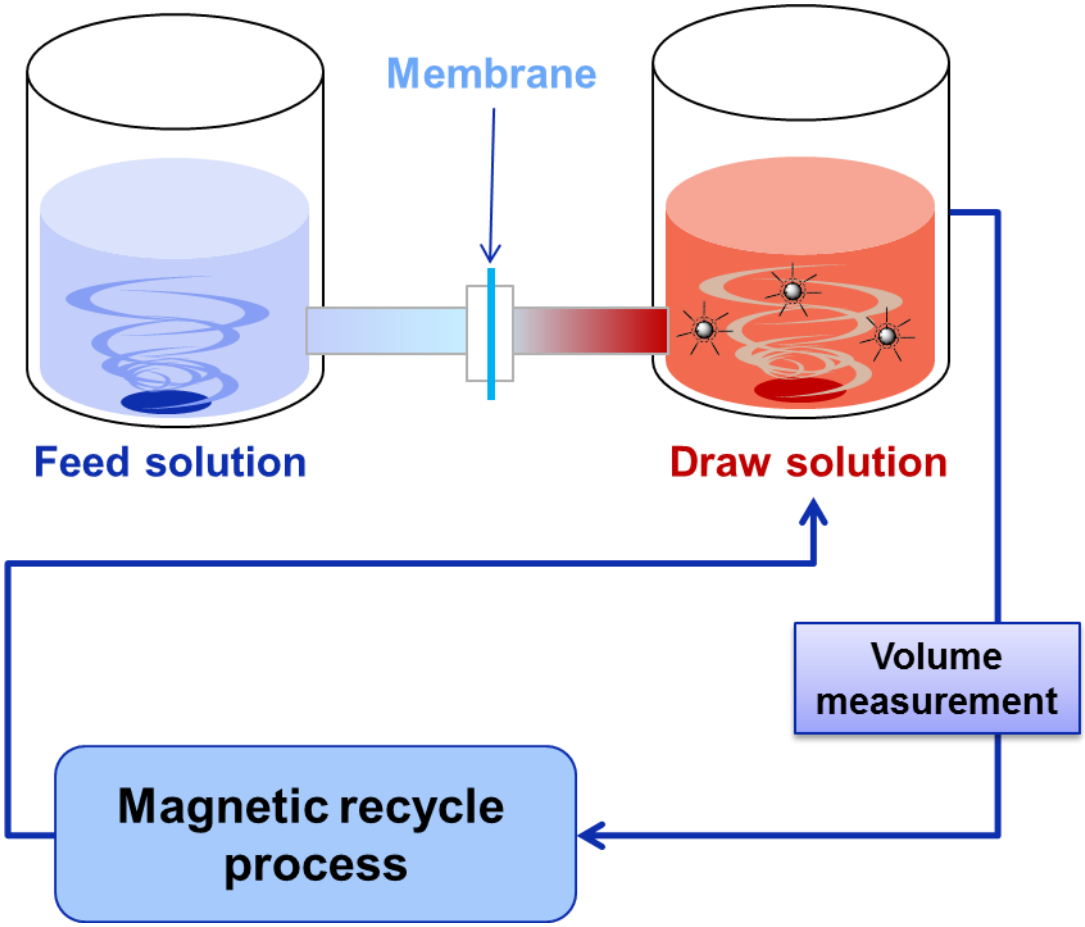

Figure 5. concept of the batch scale FO process

Table 1. experimental condition and measurement factor in FO process

Experimental condition	
Membrane	Commercialized CTA membrane (purchased from HTI)
Membrane orientation	Active layer facing feed solution
Membrane area	2.54 cm^2 (0.9 × 0.9 × π cm^2)
Feed solution	120 mL of DI water
Draw solution	120 mL of HS-MNP aqueous solution
Magnetic recycle of HS-MNP	5 times with magnet (over 13000 gauss)

Table 2. measurement factors in FO process

Measurement	
Water flux	Volume increase of draw solution each 30 minutes
	Change of water flux after each run of magnetic recycle
Particle size variation	Mean particle size after each run of magnetic recycle

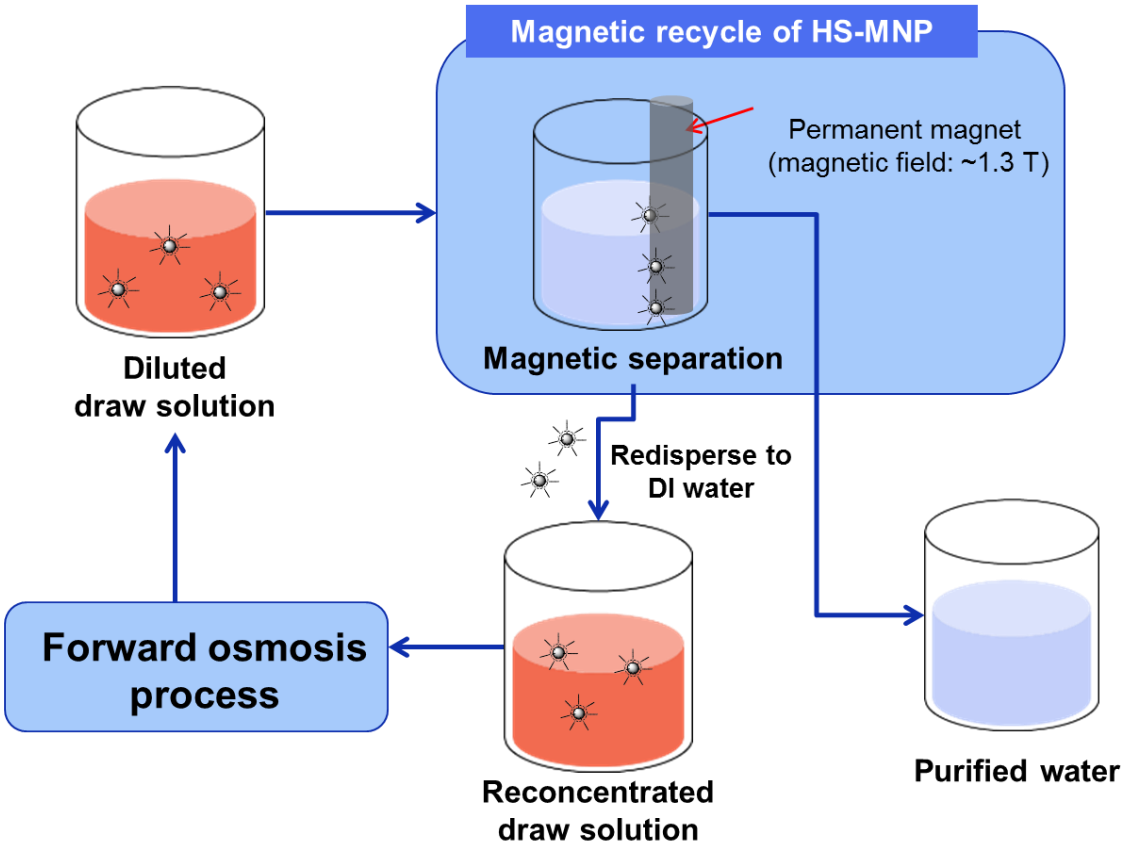

Figure 6.magnetic recycle process of HS-MNP draw solutes

3. Results and Discussion

3.1 Preparation of hydrophilic siloxane-coated magnetic nanoparticle (HS-MNP)

3.1.1. Crystal structure, shape and particle size distribution

The XRD analysis of synthesized MNP/oleic acid nanoparticles is shown in Figure 7. Results showed the well-defined reflection peaks which are similar to the characteristic peaks of magnetite (Fe_3O_4). (2 2 0), (3 1 1), (4 0 0), (4 2 2), (5 1 1), and (4 4 0) reflection peaks are considered as the evidence of successfully synthesized spinel cubic structure of magnetite (Fe_3O_4) as shown in Table 3. [31] Slightly appeared (2 1 1) reflection peak is considered as the structure of maghemite (γ-Fe_2O_3) which also have magnetic property.

Figure 8 is EF-TEM images of the MNP/oleic acid nanoparticles (dispersed in n-hexane). They show reasonable uniformity in size (5-10 nm) and shape (spherical). Figure 9 and 10 shows the EF-TEM images of HS-MNPs (both PEG-MNP and COOH-MNP were dispersed in DI water) after the hydrophilic surface modification by ligand exchange. On basis of these images, both the PEG-MNP and COOH-MNP maintained their shapes and size without any significant deformation or growth. It confirms that the modification by ligand exchange reaction affect only at the surface of the nanoparticles.

Figure 11 depicts the particle size distribution of HS-MNPs in DI water

analyzed by ELS. The ELS results show that the HS-MNPs are well dispersed in DI water. Mean particle size of PEG-MNP is 10.3 ± 2.0 nm and COOH-MNP is 13.5 ± 2.2 nm. Siloxane ligands of HS-MNPs makes the larger mean size than observed in EF-TEM images which cannot show the organic ligand molecules.

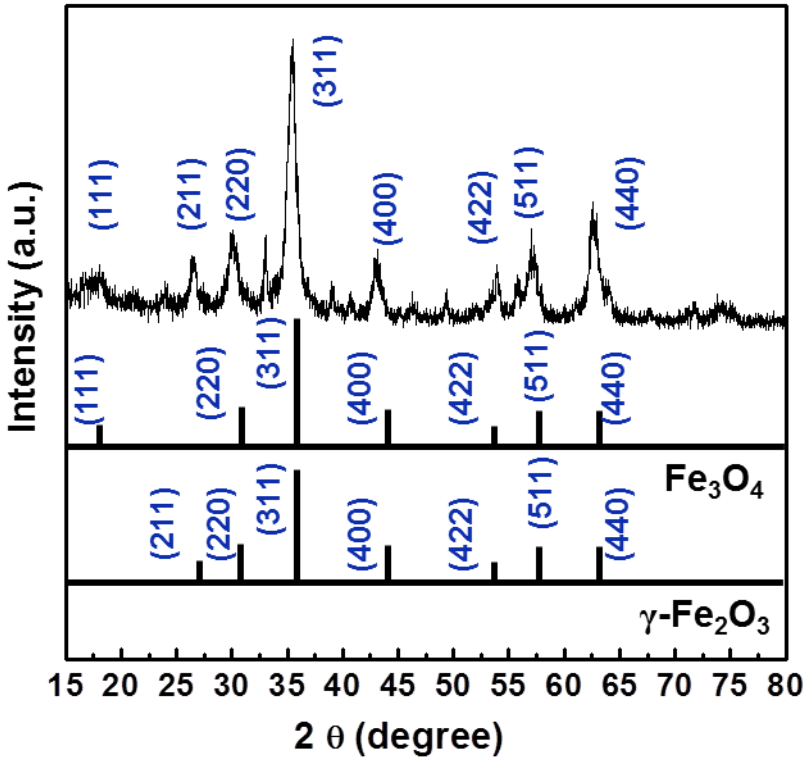

Figure 7. XRD spectra of synthesized MNP

Table 3. standard 2θ values and relative intensity for magnetite

(JCPDS file #19-0629)

2θ (degree)	intensity	h k l
18.3	8	1 1 1
30.1	30	2 2 0
35.4	100	3 1 1
37.1	8	2 2 2
43.1	20	4 0 0
53.4	10	4 2 2
56.9	30	5 1 1
62.5	40	4 4 0
65.7	2	5 3 1
70.9	4	6 2 0
73.9	10	5 3 3
75.0	4	6 2 2
78.9	2	4 4 4
86.6	4	6 4 2

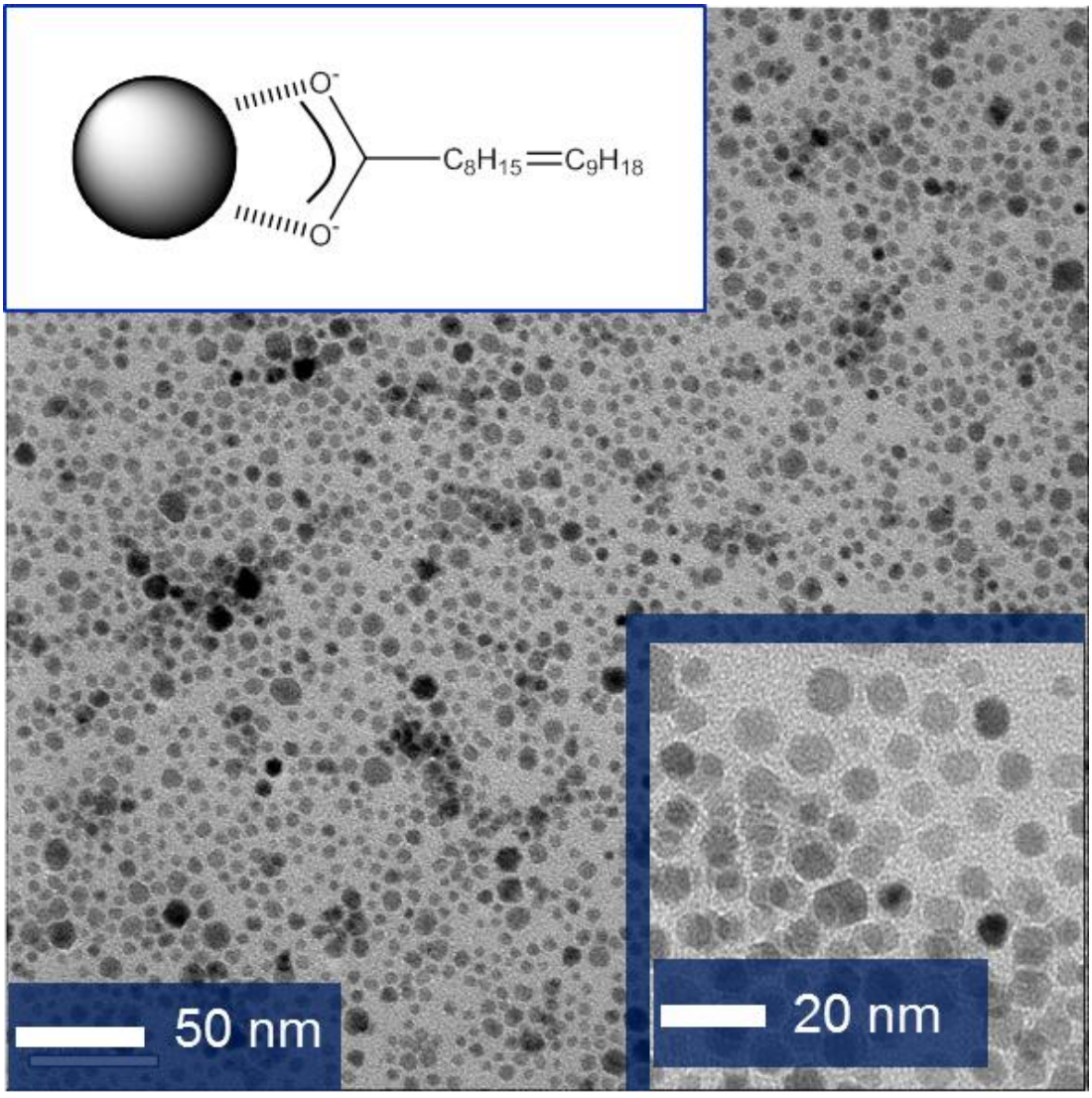

Figure 8. EF-TEM images of MNP/oleic acid nanoparticle

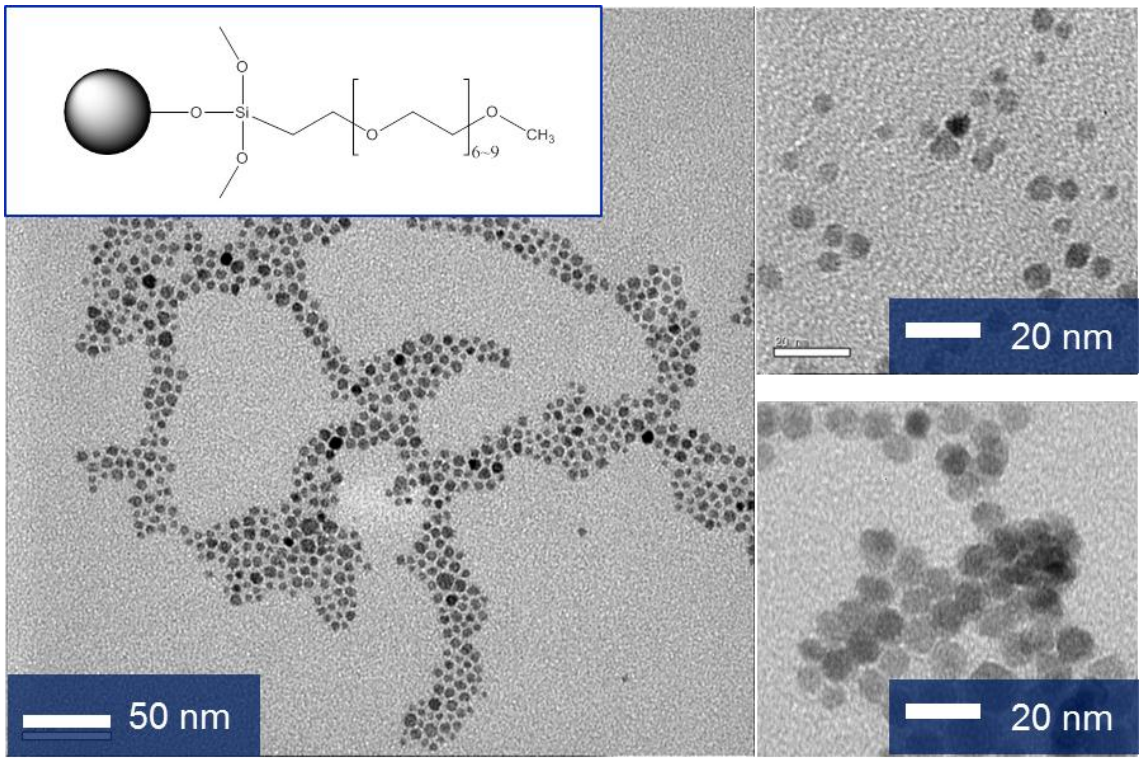

Figure 9. EF-TEM images of PEG-MNP

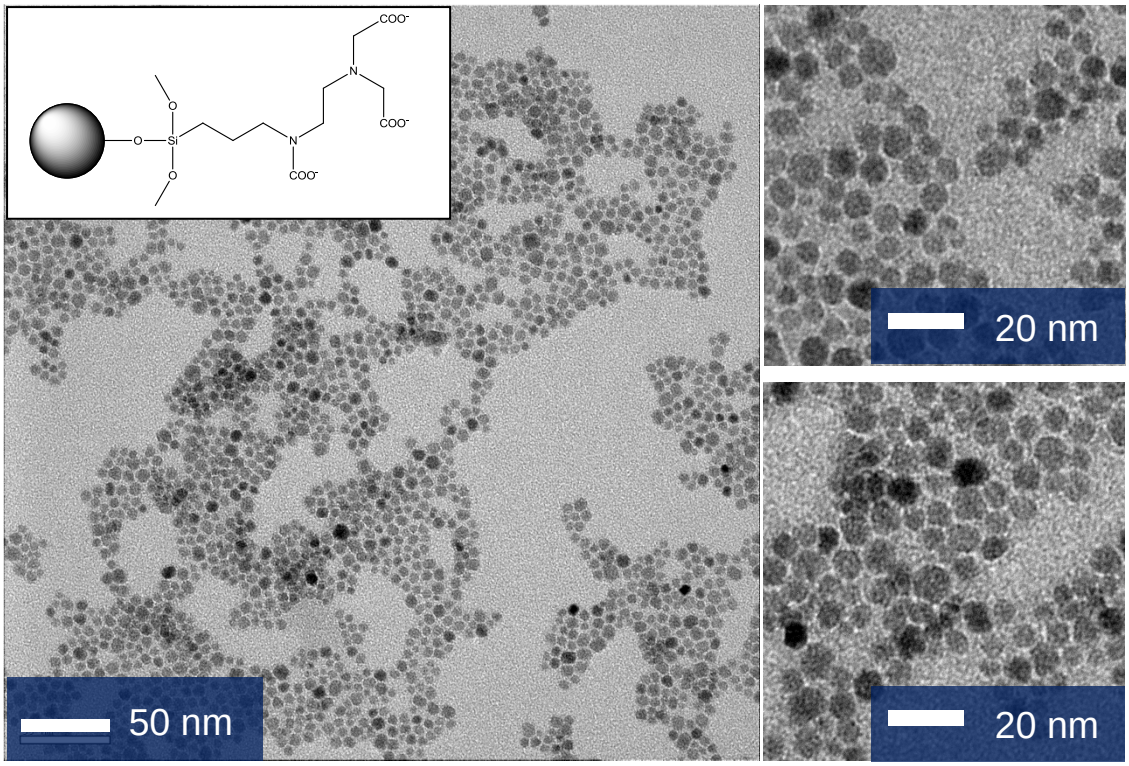

Figure 10. EF-TEM images of COOH-MNP

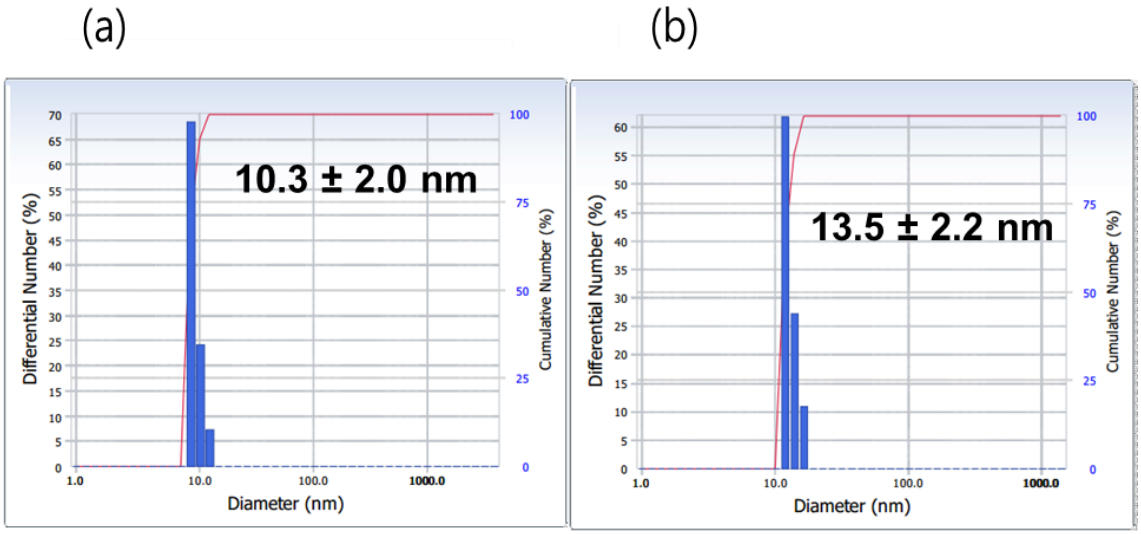

Figure 11. ELS results of the (a) PEG-MNP, and

(b) COOH-MNP dispersed in DI water

3.1.2. Surface modification by ligand exchange reaction

FT-IR spectra of the synthesized MNP/oleic acid nanoparticle and PEG-MNP are depicted in Figure 12. (a) is about the MNP/oleic acid nanoparticles before ligand exchange reaction, (b) is about a trimethoxysilane (Silane-PEG) which is added for surface modification, and (c) is about the PEG-MNP after the ligand exchange. By comparison of the Figure 12(a), (b) and (c), C=C stretch and C-H bend in MNP/oleic acid were disappeared after surface modification. In addition to, whole of the characteristic peaks of Silane-PEG: Si-O-Fe (1030 cm^{-1}), Si-C (1250 cm^{-1}), and C-O-C stretch in ethylene glycol (1040-1120 cm^{-1}) were distinctly observed after the ligand exchange reaction, and Si-O-Si (1100 cm^{-1}) stretch peak as evidence of condensation reaction of Silane-PEG was appeared in PEG-MNPs. FT-IR spectra of the COOH-MNP are similar to the PEG-MNP as shown in Figure 13. (a) is about the MNP/oleic acid nanoparticles, (b) is about a Silane-COOH, and (c) is about the COOH-MNP. After the ligand exchange reaction, characteristic peaks of oleic acid such as C=C stretch and C-H bend were disappeared, and peaks of Silane-COOH such as Si-O-Fe (1030 cm^{-1}), Si-C (1250 cm^{-1}), and C-O stretch in carboxyl functional groups (-COOH) (1320 cm^{-1}) were observed in COOH-MNP. In addition, similar to the PEG-MNP, Si-O-Si (1100 cm^{-1}) stretch was appeared after the surface modification. The whole of FT-IR spectra demonstrated that hydrophilic surface modification by ligand exchange reaction between oleic acid and hydrophilic triethoxysilanes are successfully occurred.

Figure 14 and 15 shows the results of DTA/TGA analysis which provide quantitative evidence of surface modification of HS-MNPs. The information from DTA/TGA measurements is bipartite. First of all, DTA results allow to us to determine the bonding strength of the ligand to the surface of nanoparticles and its thermal stability. Second, TGA results can offer us the quantitative data of ligand molecules which are surrounding each nanoparticle. Equation to calculate the ligand/particle ratio is shown below.

$$\mathrm{N} = \frac{\varpi N_A \rho \frac{4}{3}\pi R^3 \times 10^{-23}}{MW} \quad \text{(Eq. 3)}$$

Where N is the number of ligands on each particle (ligand/particle ratio), ω is the weight loss in percent, N_A is Avogadro's number, ρ is the density of the nanoparticles approximated as 5.0 g/cm^3, R is the mean radius of the Fe_3O_4 nanoparticles approximated as 7.0 nm based on EF-TEM images, and MW is the molecular weight of the ligand molecules (g/mol).

Typically, as the bonding of ligands and particle surface is more strongly as, they are desorbed at higher temperatures. The results of DTA are depicted in Figure 14. The MNP/oleic acid nanoparticles show a primary weight loss by boiling of oleic acid molecules at 236.70 ℃, and a second weight loss by decomposition of ligand molecules that bind to surface of nanoparticle directly at 351.90 ℃. This desorption pattern is

similar to the literature for oleic acid ligands which are already reported. [32] The third weight loss at 709.09 ℃ is derived by the phase transition (reduction) of nanoparticle core from Fe_3O_4 to FeO. After surface modification, desorption temperature of the ligand molecules are increased. In PEG-MNPs, a peak of weight loss is observed at 386.77 ℃. COOH-MNPs show peaks of weight loss at 388.25 ℃ and 449.31 ℃. This increase in desorption temperature compared to oleic acid is indicative of an increased bonding strength between ligand molecules and surface of nanoparticles by the covalent nature of the Fe-O-Si and Si-O-Si linkages.

Figure 15 shows the TGA results, and Table 4 shows the weight loss of the MNP/oleic acid, PEG-MNP, and COOH-MNP by decomposition of ligand molecules which are analyzed by TGA results. Weight loss of the ligand molecules is measured by the variance of weight (%) between before and after of the primary weight loss peaks, and ligand/particle ratio was calculated by Eq. 3. The ligand/particle ratio of PEG-MNP is calculated as 1224.42, and COOH-MNP is 1121.01. It means that 1224.42 of the Silane-PEG ligands and 1121.01 of the Silane-COOH ligands bind to one of their own Fe_3O_4 nanoparticle core. This phenomenon is explained by the molecular structure of Silane-MNP and Silane-COOH as shown in Figure 16. Silane-PEG molecules have the linear molecular structure which is favorable for efficient packing. In contrast, Silane-COOH molecules have multi-branched structure by three of carboxyl functional groups which cause the steric effect. In addition, electronic repulsion by carboxylic functional

groups of Silane-COOH can also disturb the efficient packing of ligands on particle surface.

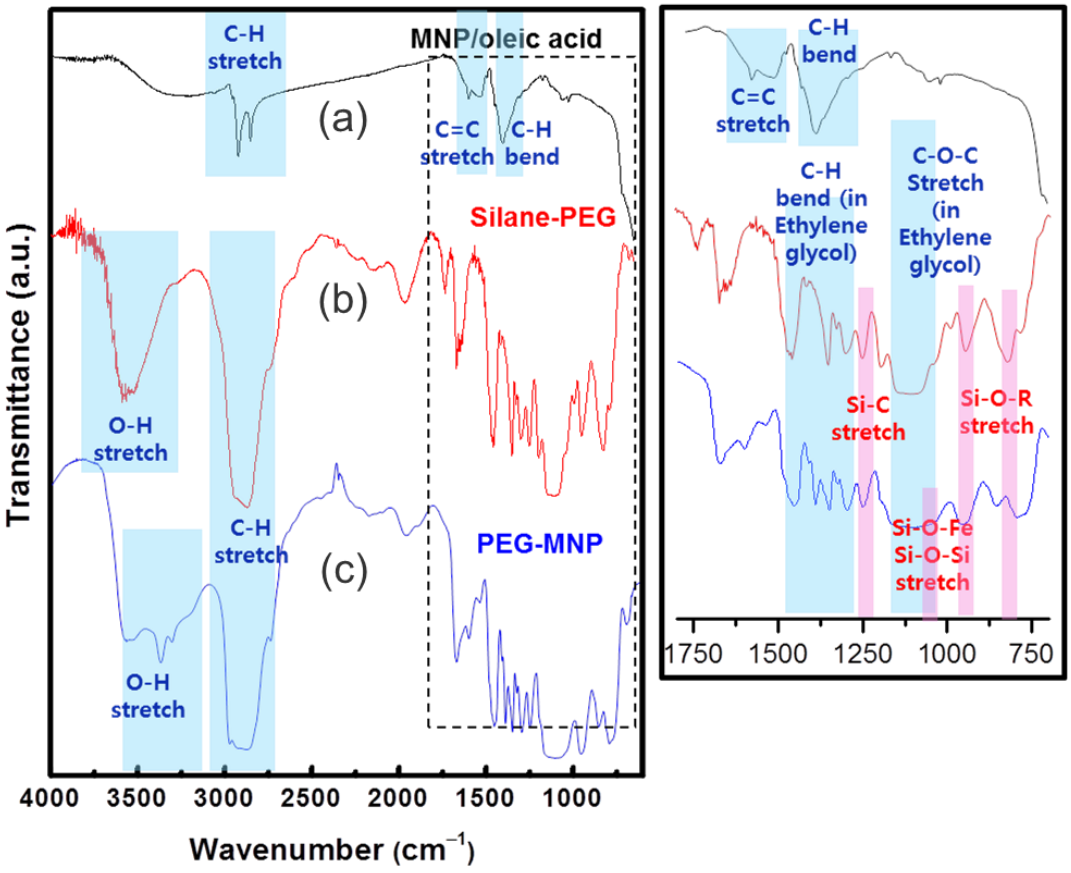

Figure 12. FT-IR spectra of the (a) MNP/oleic acid nanoparticle, (b) Silane-PEG molecules, and (c) PEG-MNP

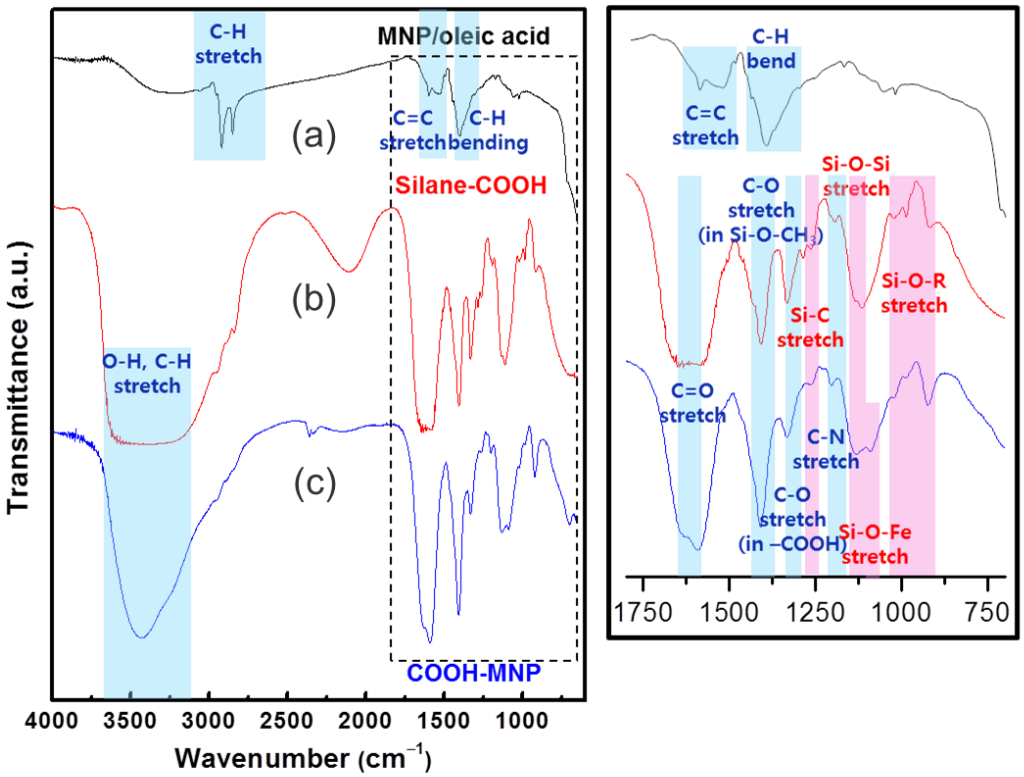

Figure 13. FT-IR spectra of the (a) MNP/oleic acid nanoparticle, (b)Silane-COOH molecules, and (c) COOH-MNP

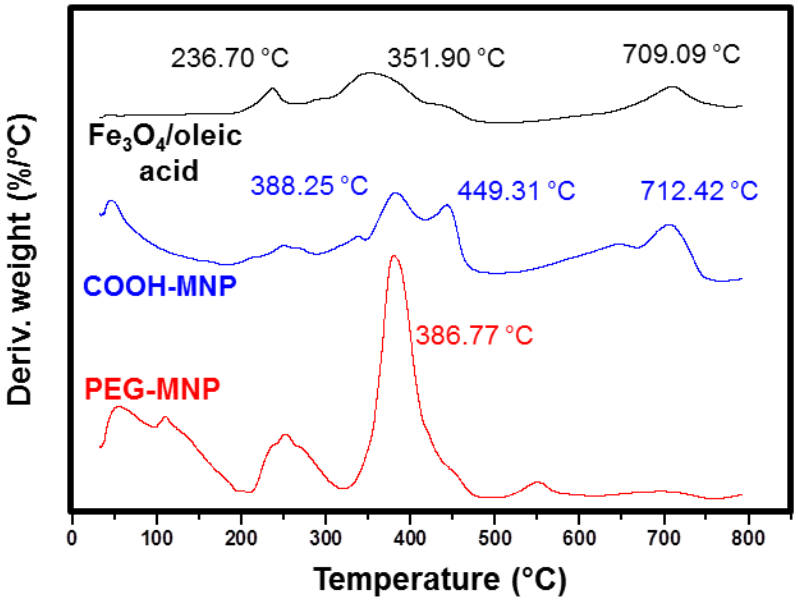

Figure 14. DTA results of MNP/oleic acid and HS-MNPs

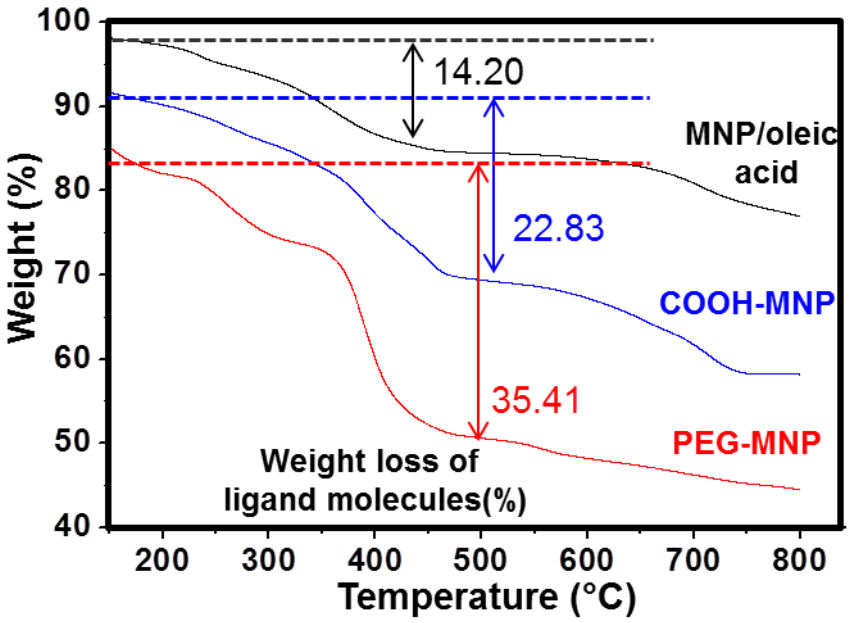

Figure 15. TGA results of MNP/oleic acid and HS-MNPs

Table 4. weight loss and ligand/particle ratio of MNP/oleic acid and HS-MNPs

Samples	Weight loss of ligands (%)	Ligand/ particle ratio
MNP /oleic acid	14.20	808.22
COOH-MNP	22.83	1121.01
PEG-MNP	35.41	1224.42

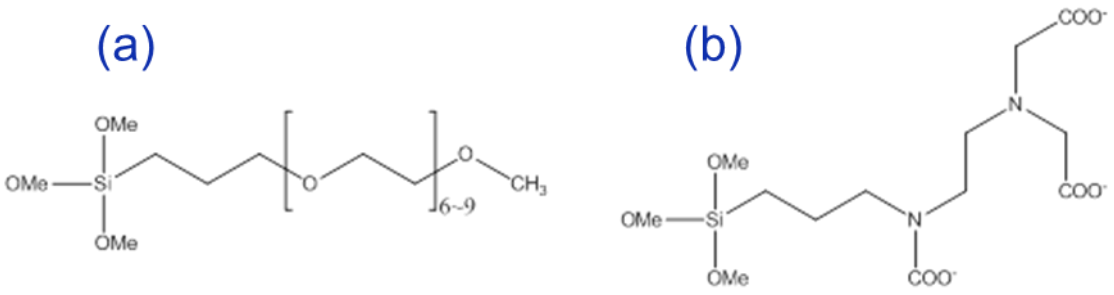

Figure 16. molecular structure of (a) Silane-PEG, and (b) Silane-COOH

3.1.3. Osmotic pressure generation

The concentration of ligand molecules surrounding each nanoparticle was directly related with the whole osmotic pressure generation of HS-MNP draw solutes. Formula for calculation of concentration of ligand molecules is shown in below. [22]

$$C = \frac{(\rho - \rho_{water}) \cdot w}{M_w}$$

Where C is the molar concentration, ρ is the density of the magnetic nanoparticle solution (g/L), ρ_{water} is the density of the water (assumed to be 1000 g/L), w is the mass percentage of the ligand upon magnetic nanoparticles (obtained by TGA analysis), and M_w is the molecular weight of the ligand molecule. It is assumed that no additional volume change is occurred in the draw solution after the addition of HS-MNPs.

Table 5 shows the osmolality of HS-MNPs dispersed in DI water analyzed by freezing point depression osmometer. Results of PEG-MNP are marked as square symbol, and COOH-MNP are marked as circle. Originally, freezing point depression osmometer can offer only the osmolality of the HS-MNPs in solution. Osmolality is a variation of molality that only takes into account solutes that contribute to a solution's

osmotic pressure. Osmotic pressure generation of HS-MNPs is calculated based on arranged Van't Hoff equation (Eq. 4) with the osmolality of HS-MNPs.

$$\pi = [B]RT \quad \text{(Eq. 4)}$$

Where π is the osmotic pressure, [B] is the osmolality of HS-MNPs in DI water, R is the gas constant, and T is the absolute temperature of the solution.

Both PEG-MNP and COOH-MNP were concentrated at 50 g/L, (calculated by Eq. 3, concentration of ligand molecules is at 0.038 mol/L) osmotic pressure generation of PEG-MNP was up to 7.6 atm, and COOH-MNP was 6.3 atm, as shown in Figure 17. At over 50 g/L, both PEG-MNP and COOH-MNP were saturated in solution and some precipitate was settled to the bottom. It is considered that the bigger ligand/particle ratio of PEG-MNP than COOH-MNP induced the larger osmotic pressure generation of PEG-MNP than COOH-MNP. Based on the osmometer analysis, synthesized HS-MNPs can be applied to FO water treatment on mild brackish water of which salinity is under 5000 ppm (its osmotic pressure is about 4 atm).

Concentration of ligand molecules (mol/L)	0.0076	0.0152	0.0228	0.0304	0.038
PEG-MNP	53	119	187	226	297
COOH-MNP	45	106	162	191	245

Table 5. osmolality of HS-MNPs

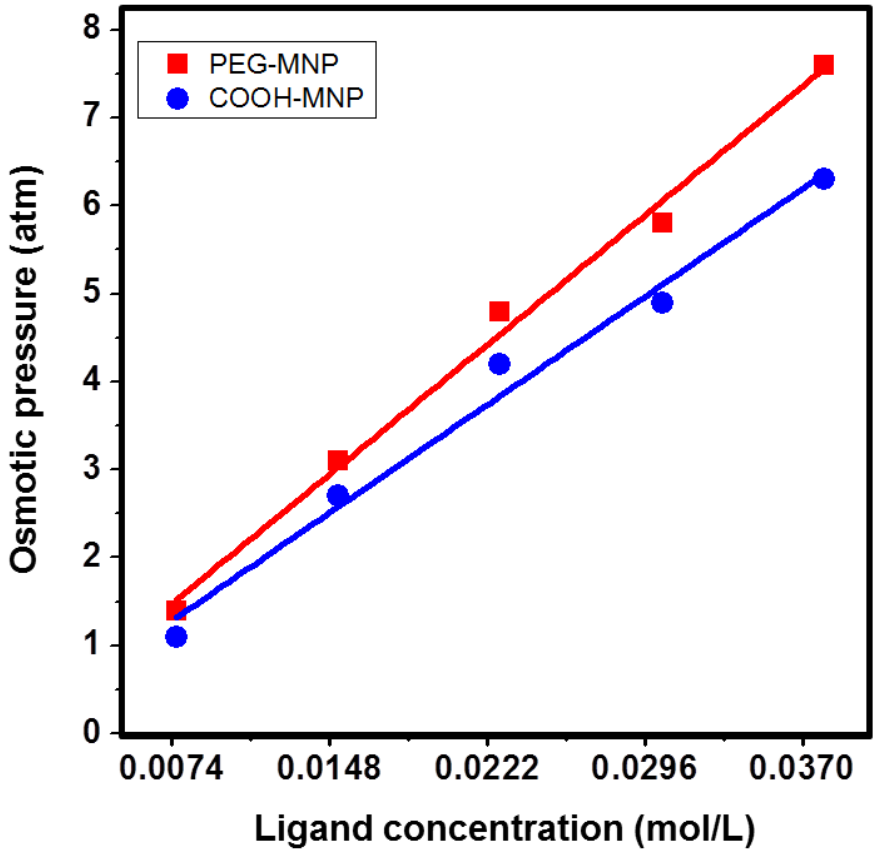

Figure 17. variation of osmotic pressure of HS-MNPs

3.2. FO process with HS-MNP draw solutes

3.2.1. Water flux of HS-MNP draw solutes with DI water feed solution

The water permeation flux, J_v (L/m^{2}h, abbreviated as LMH), is calculated from the volume change of the draw solution using below equation.

$$J_v = \Delta V / A \Delta t \quad \text{(Eq. 5)}$$

Where ΔV is the volume change of the draw solution, Δt is the predetermined time for permeation, and A is the effective membrane surface area. The volume increase by water permeation in FO process is depicted in Figure 18. With the time passed, water flux was gradually decreased because of the increased volume and diluted concentration of draw solution by dead-end FO process. Water flux generation tended to be increased with the increase of concentration of draw solution. The water flux generation of PEG-MNP draw solutes was up to 2.13 LMH at 0.038 mol/L, and COOH-MNP was 1.81 LMH at same concentration as shown in Figure 19. The results are correspondent to the osmotic pressure generation of both PEG-MNP and COOH-MNP.

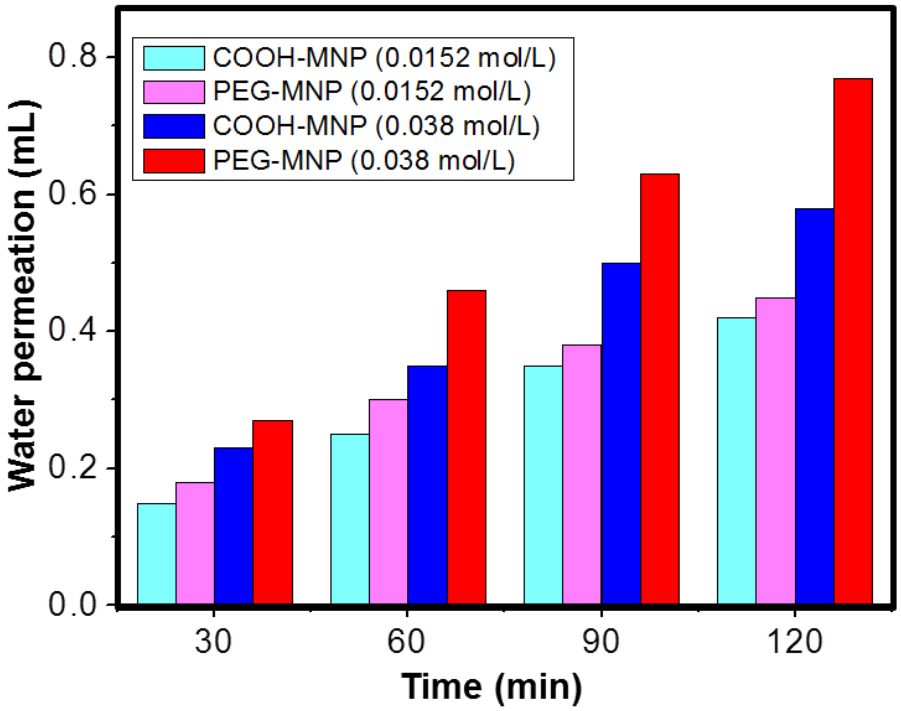

Figure 18. volume of permeated water in FO process with HS-MNPs

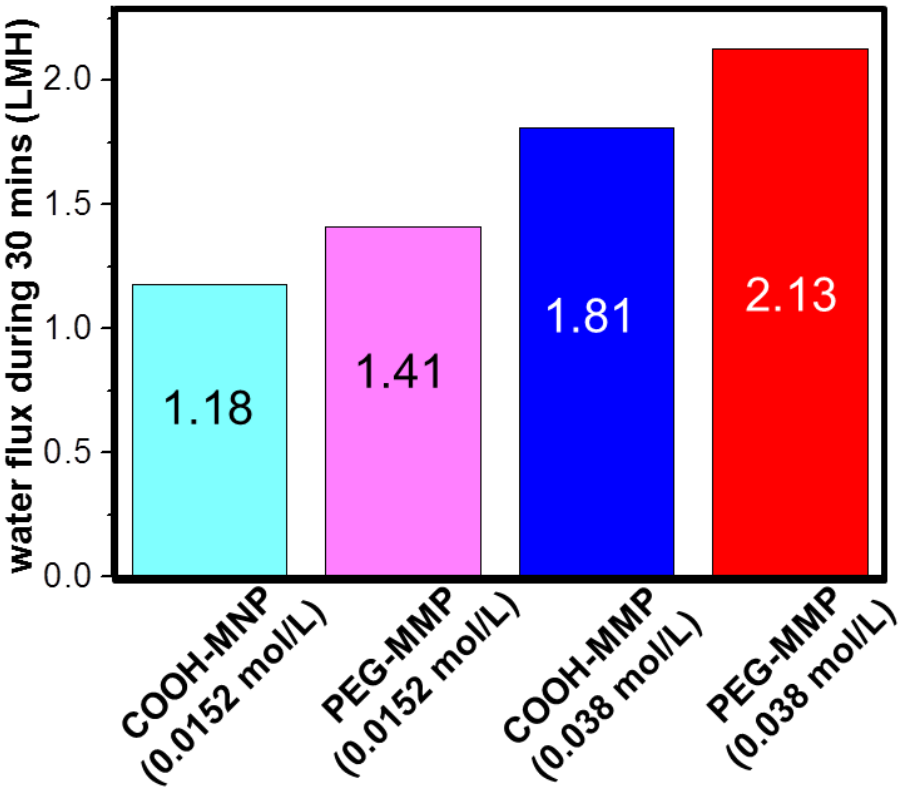

Figure 19. water flux of during 30 mins with HS-MNPs

3.2.2. Change of water flux and mean particle size in FO process on repeated magnetic recycle

Figure 20 shows the changes of HS-MNP draw solutes in terms of water flux and particle size after each recycle. The ligand concentration of HS-MNPs is maintained at 0.038 mol/L for equitable comparison. Compared with the report of Ge, Q., et al. [21], Water flux of PEG-MNP was relatively well-maintained at 2.01 ± 0.12 LMH within 10% of the baseline values. It confirms that PEG-MNP has enough particle stability to prevent the particle core aggregation during magnetic separation. However, Water flux of COOH-MNP was significantly decreased after 4th times of magnetic recycle. Particle mean size of PEG-MNP was well-maintained about 11.1 ± 0.8 nm during 5 times of magnetic recycle process. In contrast, particle mean size of COOH-MNP was maintained about 14.0 ± 0.6 nm during 3 times of recycle, but significantly increased over 90 nm after 4 times of recycle. The particle size increase of COOH-MNP is the origin of the FO performance decline after 4 times of magnetic recycle process. This problem seems to be originated by hydrogen bonding of carboxyl functional groups of COOH-MNP which can induce the particle aggregation with their hydrogen bonding by attraction among the nanoparticles.

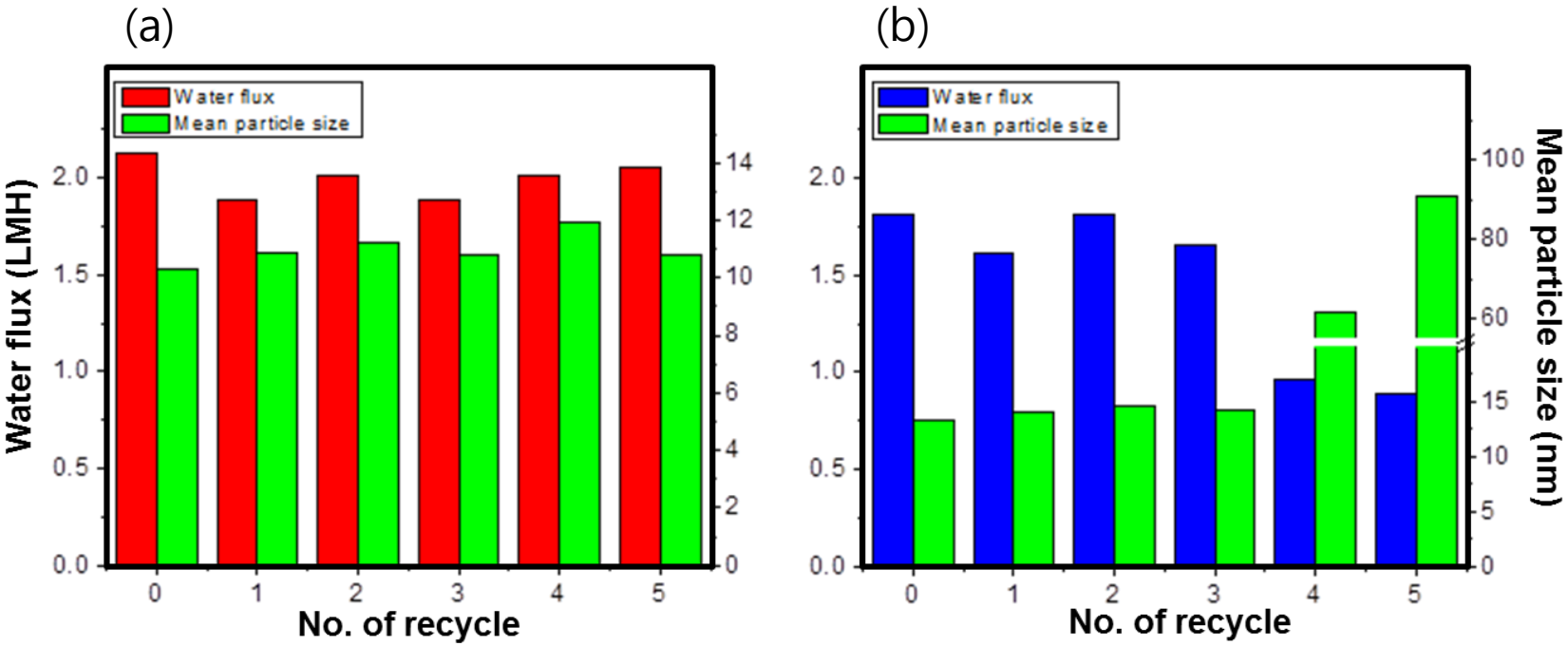

Figure 20. change of water flux and mean particle size of (a) PEG-MNP and

(b) COOH-MNP after each run of recycle

3.2.3. Water flux of PEG-MNP draw solutes with brackish feed solution

Until the results of this study, PEG-MNP was more acceptable draw solute than COOH-MNP. Finally, 0.038 mol/L of PEG-MNP draw solution was applied to the FO process with mild brackish water feed solution which was produced by addition of 500 ppm of methylene blue to the DI water. Figure 21 shows that water permeation with PEG-MNP draw solutes and brackish feed solution. Water flux was up to 1.58 LMH, which is 75% of the result with DI water feed, as shown in Figure. 22. This result confirms that PEG-MNP draw solutes can be applied to the FO water treatment of mild brackish water.

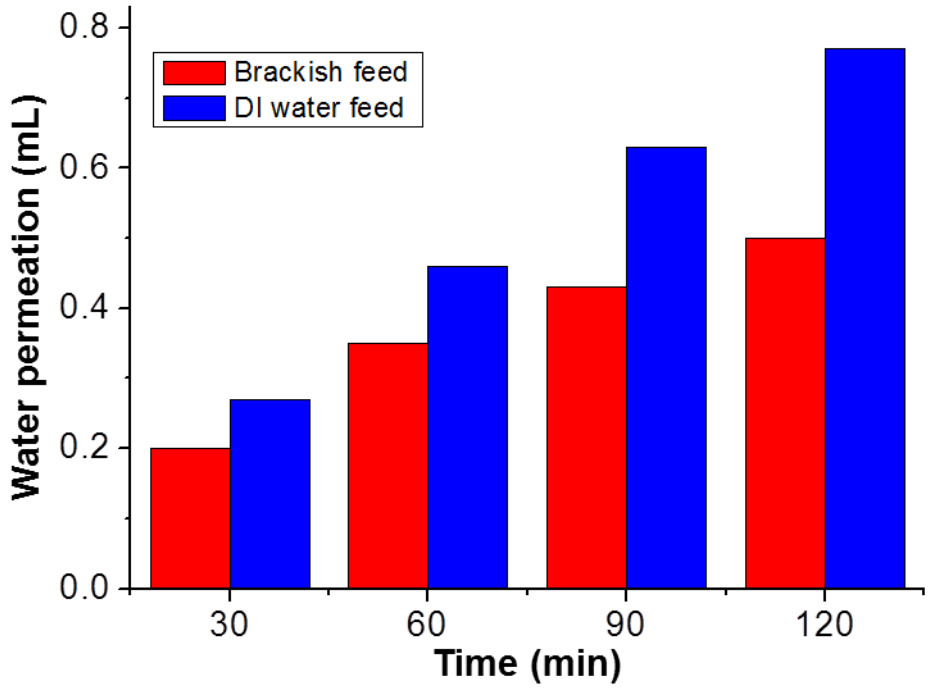

Figure 21. water flux in FO process with PEG-MNP draw solution and 500 ppm of methylene blue feed solution

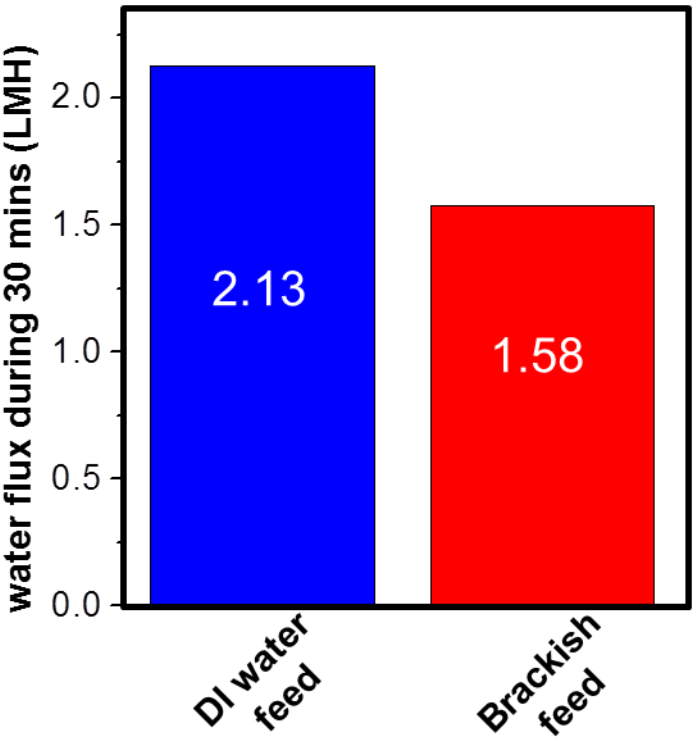

Figure 22. water flux in FO process with PEG-MNP draw solution and 500 ppm of methylene blue feed solution

4. Conclusions

In this study, hydrophilic siloxane-coated magnetic nanoparticle (HS-MNP) draw solutes were synthesized and applied to the FO process. Several conclusions have been determined as the follow.

1. Hydrophilic silane-capped magnetic nanoparticles (HS-MNPs) are synthesized by ligand exchange reaction between oleic acid and hydrophilic silane. The evidence of surface modification with hydrophilic siloxane is derived from the results of the FT-IR spectra and DTA/TGA analysis. All of the HS-MNPs have spherical shapes. Particle mean size of PEG-MNPs is 5-10 nm based on EF-TEM images, and 10.3 ± 1.3 nm based on ELS analysis. COOH-MNP is 5-10 nm based on EF-TEM, and 13.5 ± 1.6 nm based on ELS.

2. Ligand/particle ratio of synthesized HS-MNPs was calculated by results of TGA analysis. Ligand/particle ratio of PEG-MNP is 1224.42, and COOH-MNP is 1121.01. This phenomenon is explained by the molecular structure of Silane-MNP and Silane-COOH. Silane-PEG molecules have the linear

molecular structure which is favorable for efficient packing. In contrast, Silane-COOH molecules have multi-branched structure and electronic repulsion by carboxylic functional groups which are unfeasible for packing.

3. Osmotic pressure generation of HS-MNPs was calculated by results of osmometer analysis. PEG-MNPs have 7.6 atm of osmotic pressure at 50 g/L (ligand concentration is 0.038 mol/L), and COOH-MNPs have the 6.3 atm at same concentration. Based on this results, HS-MNPs can be applied to FO water treatment of brackish water which are concentrated up to 5000 ppm.

4. By applying to the batch scale FO process, water flux generation of HS-MNP draw solutes are measured. PEG-MNPs generated up to 2.13 LMH of water flux at 0.038 mol/L, and COOH-MHP generated 1.81 LMH at same concentration. Although the Silane-COOH molecules are more hydrophilic than Silane-PEG, generated osmotic pressure of PEG-MNP are larger than COOH-MNP. It may be originated by the ligand/particle ratio of PEG-MNP is bigger than COOH-MNP.

5. Water flux of PEG-MNP draw solute was relatively well-maintained within 2.01 ± 0.12 LMH through 5 runs of magnetic recycle. Variation of particle mean size was within 11.1 ± 0.8 nm. It confirms that PEG-MNP has enough particle stability to prevent the particle core aggregation during magnetic separation. However, Water flux of COOH-MNP was significantly decreased after 4th times of magnetic recycle. It is originated by the particle aggregation of COOH-MNP. Based on ELS analysis, particle mean size of COOH-MNP was maintained about 14.0 ± 0.6 nm during 3 times of recycle, but significantly increased over 90 nm after 4 times of recycle. It seems that this results is originated by molecular structure of Silane-COOH, the ligands of the COOH-MNP.

6. The water flux in FO process with 0.038 mol/L of PEG-MNP draw solute and 500 ppm of methylene blue feed solute was up to 1.58 LMH. It confirms that PEG-MNP draw solute was feasible to the FO water treatment with the mild brackish water as feed solution.

In conclusion, hydrophilic siloxane-capped magnetic nanoparticles were

successfully synthesized. And, as feasible hydrophilic magnetic nanoparticle draw solutes, confirmed to apply to FO process for water treatment for mild brackish water. In addition, PEG-MNP is demonstrated that it has the enough stability to maintain its FO performance during the magnetic separation process, and feasible water flux generation in FO process of brackish water.

5. References

1. Montgomery, M.A. and M. Elimelech, *Water and sanitation in developing countries: including health in the equation.* Environmental Science & Technology, 2007. **41**(1): p. 17-24.

2. Shannon, M.A., et al., *Science and technology for water purification in the coming decades.* Nature, 2008. **452**(7185): p. 301-310.

3. Ge, Q., et al., *Exploration of polyelectrolytes as draw solutes in forward osmosis processes.* Water research, 2011.

4. Fritzmann, C., et al., *State-of-the-art of reverse osmosis desalination.* Desalination, 2007. **216**(1): p. 1-76.

5. Cath, T.Y., A.E. Childress, and M. Elimelech, *Forward osmosis: Principles, applications, and recent developments.* Journal of Membrane Science, 2006. **281**(1): p. 70-87.

6. Van der Bruggen, B., L. Lejon, and C. Vandecasteele, *Reuse, treatment, and discharge of the concentrate of pressure-driven membrane processes.* Environ Sci Technol, 2003. **37**(17): p. 3733-8.

7. McCutcheon, J.R., R.L. McGinnis, and M. Elimelech, *A novel ammonia—carbon dioxide forward (direct) osmosis desalination process.* Desalination, 2005. **174**(1): p. 1-11.

8. Chung, T.-S., et al., *Forward osmosis processes: Yesterday, today and tomorrow.* Desalination, 2012. **287**(0): p. 78-81.

9. Kessler, J. and C. Moody, *Drinking water from sea water by forward osmosis.* Desalination, 1976. **18**(3): p. 297-306.

10. Choi, Y.J., et al., *Toward a combined system of forward osmosis and reverse osmosis for seawater desalination.* Desalination, 2009. **247**(1): p. 239-246.

11. Anderson, D.K., *Concentration of dilute industrial wastes by direct osmosis*, 1977, University of Rhode Island.

12. Kim, Y.C. and M. Elimelech, *Potential of osmotic power generation by pressure retarded osmosis using seawater as feed solution: Analysis and experiments.* Journal of Membrane Science, 2013. **429**(0): p. 330-337.

13. Phuntsho, S., et al., *A novel low energy fertilizer driven forward osmosis desalination for direct fertigation: Evaluating the performance of fertilizer draw solutions.* Journal of Membrane Science, 2011. **375**(1): p. 172-181.

14. Petrotos, K.B., P.C. Quantick, and H. Petropakis, *Direct osmotic concentration of tomato juice in tubular membrane – module configuration. II. The effect of using clarified tomato juice on the process performance.* Journal of Membrane Science, 1999. **160**(2): p. 171-177.

15. Phuntsho, S., et al., *A novel low energy fertilizer driven forward osmosis desalination for direct fertigation: Evaluating the performance of fertilizer draw*

solutions. Journal of Membrane Science, 2011. **375**(1-2): p. 172-181.

16. Achilli, A., T.Y. Cath, and A.E. Childress, *Selection of inorganic-based draw solutions for forward osmosis applications.* Journal of Membrane Science, 2010. **364**(1-2): p. 233-241.

17. Yokozeki, A., *Osmotic pressures studied using a simple equation-of-state and its applications.* Applied energy, 2006. **83**(1): p. 15-41.

18. Chekli, L., et al., *A review of draw solutes in forward osmosis process and their use in modern applications.* Desalination and Water Treatment, 2012. **43**(1-3): p. 167-184.

19. Tan, C. and H. Ng, *A novel hybrid forward osmosis-nanofiltration (FO-NF) process for seawater desalination: Draw solution selection and system configuration.* Desalination and Water Treatment, 2010. **13**(1-3): p. 356-361.

20. McCutcheon, J.R., R.L. McGinnis, and M. Elimelech, *Desalination by ammonia–carbon dioxide forward osmosis: Influence of draw and feed solution concentrations on process performance.* Journal of Membrane Science, 2006. **278**(1): p. 114-123.

21. Ge, Q., et al., *Hydrophilic Superparamagnetic Nanoparticles: Synthesis, Characterization, and Performance in Forward Osmosis Processes.* Industrial & Engineering Chemistry Research, 2010. **50**(1): p. 382-388.

22. Ling, M.M., K.Y. Wang, and T.S. Chung, *Highly Water-Soluble Magnetic*

Nanoparticles as Novel Draw Solutes in Forward Osmosis for Water Reuse. Industrial & Engineering Chemistry Research, 2010. **49**(12): p. 5869-5876.

23. Ling, M.M., T.S. Chung, and X. Lu, *Facile synthesis of thermosensitive magnetic nanoparticles as "smart" draw solutes in forward osmosis.* Chemical Communications, 2011. **47**(38): p. 10788-10790.

24. Ling, M.M. and T.S. Chung, *Desalination process using super hydrophilic nanoparticles via forward osmosis integrated with ultrafiltration regeneration.* Desalination, 2011. **278**(1): p. 194-202.

25. Sun, Y., et al., *Magnetic separation of polymer hybrid iron oxide nanoparticles triggered by temperature.* Chemical communications, 2006(26): p. 2765-2767.

26. Pena-Pereira, F., R.M.B.O. Duarte, and A.C. Duarte, *Immobilization strategies and analytical applications for metallic and metal-oxide nanomaterials on surfaces.* TrAC Trends in Analytical Chemistry, 2012. **40**(0): p. 90-105.

27. Sun, S., et al., *Monodisperse MFe2O4 (M = Fe, Co, Mn) Nanoparticles.* Journal of the American Chemical Society, 2003. **126**(1): p. 273-279.

28. De Palma, R., et al., *Silane Ligand Exchange to Make Hydrophobic Superparamagnetic Nanoparticles Water-Dispersible.* Chemistry of Materials, 2007. **19**(7): p. 1821-1831.

29. Larsen, E.K.U., et al., *Size-dependent accumulation of PEGylated silane-coated magnetic iron oxide nanoparticles in murine tumors.* ACS nano, 2009. **3**(7): p.

1947-1951.

30. Barrera, C., A.P. Herrera, and C. Rinaldi, *Colloidal dispersions of monodisperse magnetite nanoparticles modified with poly (ethylene glycol).* Journal of colloid and interface science, 2009. **329**(1): p. 107-113.

31. Si, S., et al., *Magnetic Monodisperse Fe3O4 Nanoparticles.* Crystal Growth & Design, 2005. **5**(2): p. 391-393.

32. Sahoo, Y., et al., *Alkyl Phosphonate/Phosphate Coating on Magnetite Nanoparticles: A Comparison with Fatty Acids.* Langmuir, 2001. **17**(25): p. 7907-7911.

국문초록

정삼투 (FO) 기술은 현재 분리막을 이용한 수처리 기술 중 가장 주목받고 있는 분야 중 하나이다. 특히 이러한 FO 수처리에 적합한 유도물질을 개발하는 것은 FO 연구에 있어서 가장 중요한 주제로 지목되고 있는 사항이다. 유도물질에 가장 필요한 특징 두 가지는 높은 삼투압 유도 능력과, 유도용액에서의 손쉬운 분리 및 재사용성이다. 이러한 점으로 미루어볼 때, 친수성 자성입자 (HMNP) 는 유도물질로서 적합한 특성을 갖추고 있다 할 수 있다. 그러나 자성분리가 계속됨에 따라 친수성 자성입자의 뭉침 현상으로 인하여 삼투 성능이 점차적으로 감소하는 현상이 중요한 단점으로 지목되고 있다. 이런 문제를 해결하기 위하여, 이 연구에서는 친수성 실록산을 리간드로 이용한 친수성 자성입자 유도물질 (HS-MNP) 을 합성하였다. 친수성 trimethoxysilane 분자 사이의 축합반응을 이용하여 만들어진 실록산 리간드의 공유결합은 기존 친수성 자성입자 유도물질에 주로 사용된 carboxylate 리간드의 이온성 결합에 비해 더 안정적이고 강력한 결합으로써, 이를 통해 입자들의 뭉침 현상을 방지하는 효과가 있을 것으로 기대된다. 우선, Thermal decomposition 방식으로 합성된 MNP/oleic acid 의 oleic acid 리간드를 친수성 trimethoxysilane 으로 치환하는 반응을 통하여 HS-MNP 유도물질을 합성하였다. 이 반응에는 2-[methoxy-(polyethyleneoxy)propyl] trimethoxysilane (Silane-PEG) 과, n-

(trimethoxysilylpropyl) ethylenediamine triacetic acid (Silane-COOH) 을 친수성 리간드로써 사용하였다. 합성된 HS-MNP 의 여러 특성에 대해 다양한 방법을 동원하여 분석을 진행하였고, 특히 삼투압 유도 성능을 freezing point depression osmometer 를 이용하여 측정하였다. 이렇게 합성된 HS-MNP 유도물질은 실제 배치로 스케일의 정삼투에 적용해 봄으로써 수투과 유도 성능을 측정하였고, 정삼투 과정 이후에는 HS-MNP 를 반복되는 자성 분리 과정에 적용하여 이에 따르는 HS-MNP 의 수투과 유도 성능 변화 및 입자 크기 변화를 측정하였다. 그 결과, PEG-MNP 의 경우는 0.038 mol/L 리간드 농도에서 7.6 atm 의 삼투압 유도 성능과 2.13 LMH 의 수투과 유도 성능을 보였고고, COOH-MNP 는 같은 농도에서 삼투압 6.3 atm, 수투과도 1.81 LMH 를 보였다. 이 결과는 합성된 HS-MNP 유도물질이 mild brackish water 에 대한 FO 수처리 분야에 적용될 수 있다는 가능성을 시사하였다. 특히, PEG-MNP 의 경우는 5 회에 걸쳐 반복된 자성분리 이후에도 수투과 유도 성능이 떨어지는 경향 없이 일정한 수준을 유지하였으며, 입자 크기 변화도 관측되지 않을 정도의 입자 안정성을 갖추었음을 알 수 있었다. 마지막으로, 0.038 mol/L 농도의 PEG-MNP 유도물질을 1000 ppm 농도의 메틸렌 블루를 Feed solution 으로써 사용한 FO 에 적용하여 수투과 유도능력을 측정한 결과 1.58 LMH 의 수투과도를 얻었다. 이러한 결과로써, HS-MNP 는 실제 FO 수처리에 적용될 수 있는 충분한 가능성을 갖춘 유도물질이라는 것을 알 수 있었으며, 그 중에서도

특히 PEG-MNP 는 충분한 입자 안정성을 갖춤으로써 반복되는 자성 분리 과정 하에서도 유도물질로서의 성능을 우수하게 유지하였으며, 실제 mild brackish water 의 수처리 과정에도 충분히 적용할 수 있는 삼투압 유도 성능을 갖추었음을 알 수 있었다.

감사의 글

석사학위논문을 완성하면서, 우선 무엇보다도 저를 이 자리에 있게 해 주시고, 제가 살아온 기간 동안 내내 저를 보살펴주시고 믿어주신 어머니께 깊은 감사를 드립니다.

지난 2 년간의 석사과정 기간 동안 제가 가장 많이 느낀 것은 "나는 이토록 준비가 부족한 사람이었구나" 하는 자기반성이었습니다. 공부도 마음가짐도 모자란 제가 무사히 석사학위논문을 작성할 수 있었던 것은 무엇보다도 2 년 동안 아낌없는 관심으로 지도해주신 곽승엽 교수님 덕분입니다. 진심으로 감사 드립니다. 그리고 바쁘신 와중에도 논문심사에 시간을 내어주신 장지영 교수님과 안철희 교수님께도 감사 드립니다.

또한 실험실 동료들의 조언과 격려와 협조가 없었더라면 이 석사논문은 있을 수 없었을 것입니다. 바쁘신 와중에도 연구실에 찾아오셔서 저를 포함하여 후배들에게 많은 조언과 도움을 주신 정재우 박사님, 졸업하시기 전까지 제 연구주제에 많은 영감을 주신 유병용 박사님, 외부에서 열심히 연구하는 모습을 보여주신 성학이형, 실험실 생활의 마음가짐에 언제나 귀감이 되어주신 수열이형, 제 연구 테마에 가장 많은 조언을 주신 형구형, 실험실에서의 긍정적인 마음가짐을 가르쳐주신 현중이형, 실험하는 방법도 잘 모르던 제게 많은 조언과 도움을 주신 성용이형과 우혁이형께 진심 어린 감사를 전합니다. 그리고 친해지고

싶었는데 금방 졸업해버린 치형이와 신영이에게 감사와 함께 아쉬움을 전하고, 아는 건 없는 주제에 나이만 더 먹은 후배 데리고 일하느라 있는 고생 없는 고생 다 한 지훈이, 태선이, 지환이, 지금은 졸업한 범진이에게 특별히 더 감사하며, 언제나 느긋하고 여유로운 모습이 눈부신 실험실 동기 규원이, 성실하고 마음가짐이 굳은 준호와 민영이, 생각 깊고 재능 많은 승희에게도 마찬가지로 감사의 마음을 전하고자 합니다. 마지막으로 제 석사과정 2 년 동안 제 삶에 따뜻한 관심을 보여준 모든 분들께 감사를 전하며 이만 감사의 글을 마치고자 합니다.

2013 년 2 월

안 효 원